Protective and Toxic Proteins in Alzheimer's Disease

MSc Thesis 2012

Maj Schneider Thomsen
Medicine with Industrial Specialization, Aalborg University

Title: Protective and Toxic Proteins in Alzheimers Disease

Project Period: August 2012 – 1st of June 2012

Project Group: 946, Biomedicine

Maj Schneider Thomsen

_____

Supervisors:
Associate Professor Meg Duroux, Department of Health Science and Technology, Aalborg University, Denmark and Professor Warren Tate, Biochemistry Department, University of Otago, New Zealand

Numbers Printed: 4

Pages: 55

Appendix: 5

Finished: 01.06.2012

Preface

The present master's thesis was carried out in collaboration with Professor Warren Tate, at The University of Otago, New Zealand in the period from August 2011 till May 2012. I would like to express my gratitude to Professor Warren Tate for welcoming me in his lab and for the advice and guidance throughout the project. Moreover, a huge thank to all the people in the Tate lab, and especially laboratory assistant Christina Edgar for help with general lab work and laboratory assistant Katie Bourne for the help with the production of Aβ.
I would also like to thank my supervisor at Aalborg University Associate Professor Meg Duroux, who has establishing the contact with Professor Warren Tate.
Furthermore, I would like to thank Augustinus Fonden, Den Obelske familiefond, and Oticon for economical support.

Table of contents

Abbreviations:

AD: Alzheimer's disease

AICD: APP intracellular domain

APLP: Amyloid precursor-like protein

APP: Amyloid precursor protein

Aβ: Amyloid beta

BCA: Bicinchoninic acid

BSA: Bovine serum albumin

FAD: Familial Alzheimer's disease

FPLC: Fast protein liquid chromatography

GST: Glutathione S-transferase

IPTG: Isopropyl β-D-1-thiogalactopyranoside

LTP: Long-term potentiation

MBP: Maltose binding protein

RPC: Reverse phase chromatography

sAPP*α*: Secreted amyloid precursor protein alpha

sAPPβ: Secreted amyloid precursor protein beta

Abstract

Background: Secreted amyloid precursor protein alpha (sAPPα) is a neurotropic and neuroprotective protein released after cleavage of amyloid precursor protein (APP). Cleavage of APP can also lead to the release of secreted amyloid precursor protein beta (sAPPβ) and amyloid beta (Aβ), which is postulated to be the primary neurotoxin in Alzheimers Disease (AD). The single difference between sAPPα and sAPPβ is 16 extra amino acids at the C-terminus of sAPPα. These 16 amino acids are of special interest since they also form the N-terminus of Aβ. Therefore, it was hypothesized that sAPPα and Aβ might interact.

Method/Results: A GST pull-down assay was performed with bait GST-sAPPα or GST-sAPPβ immobilized to glutathione Sepharose 4B beads and $Aβ_{1-42}$ added as prey. Subsequent, Western blot and densitometry analysis revealed significantly more binding of $Aβ_{1-42}$ by GST-sAPPα compared to GST-sAPPβ. This indicates that sAPPα interacts with $Aβ_{1-42}$ through the 16 amino acids at the C-terminus. To further characterize the interaction, five GST tagged sAPPα variants with mutations in the critical 16 amino acid region (K612A, K612V, D608-612, D602-612, and H609/10A) were constructed as well as one within a motif (RER328-330AAA) of much functional interest. The pull-down assay was repeated with the GST tagged sAPPα variants as bait and $Aβ_{1-42}$ as prey. All the sAPPα variants except K612A significantly reduced the binding of $Aβ_{1-42}$ compared to sAPPα. This further implies that the interaction between $Aβ_{1-42}$ and sAPPα is through the 16 amino acids at the C-terminus of sAPPα.

Discussion/Conclusion: sAPPα has previously been shown to protect cell cultures against Aβ induced toxicity and the finding that sAPPα interacts with Aβ may contribute to the neuroprotective effect of sAPPα by keeping sAPPα and Aβ in equilibrium.

1 Introduction

1.1 What is Alzheimer's disease?

Alzheimer's disease (AD) is a neurodegenerative disorder characterized by a gradual loss or decline in memory and other cognitive functions [Holtzman *et al.*, 2011]. It is estimated that 70-80.000 people in Denmark suffer from dementia and that AD contributes to approximately 60 % of all dementia cases [Alzheimerforeningen].

The time course of AD averages 7 to 10 years, and it will inevitably cause death. AD usually initiates with impaired recent memory, sometimes in the coexistence with changes in attention and problem-solving abilities. Then, as the disease progresses, language dysfunction, visuospatial difficulty, loss of insight, and personality changes become apparent. When the severe stage of AD is reached, the person is completely dependent on caregivers for all activities of daily living. In the advanced stage the person often becomes mute, nonambulatory, immobile, and unable to swallow or control bladder and bowel function. [Holtzman *et al.*, 2011]

Age is one of the most evident risk factors for AD, and since we are living in a time with a growing elderly population could we possible be facing an AD epidemic [Gabelle *et al.*, 2010]. It is estimated in the World Alzheimer Report 2010 that dementia has a worldwide cost of US$604 billion currently, and that 36 million people worldwide are living with dementia, with the number of cases expected to double every 20. [Wimo and Prince, 2010] At the

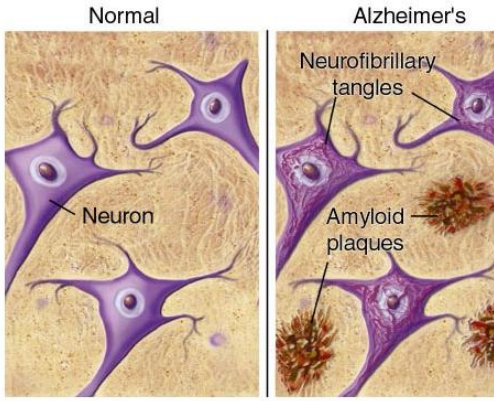

Figure 1: Schematic illustration of the neurofibrillary tangles and amyloid plaques in AD. [American-Health-Assistance-Foundation, 2000-2012]

moment no cure or effective treatment is available and so research into the disease is of the paramount importance.

The pathological hallmarks of AD are (i) extracellular amyloid plaques, which primarily are composed of amyloid beta (Aβ) peptide, and, (ii) intracellular neurofibrillary tangles composed of hyperphosphorylated tau protein, see Figure 1. [Holtzman *et al.*, 2011]

Familial AD (FAD) represents <1 % of AD cases and is inherited in an autosomal dominant fashion. FAD arises from mutations in genes, which are involved in the production of Aβ, leading to its accumulation. In the remaining 99 % of the cases an accumulation of Aβ is also seen, however the underlying reason for this remains unclear and the cases are often referred to as sporadic AD. [Marsden *et al.*, 2011; Holtzman *et al.*, 2011]

The first gene which was identified to have mutations causing the familial form, FAD, was amyloid precursor protein (APP). APP is the protein that by sequential proteolysis can generate Aβ. Later mutations in the enzymes involved in the cleavage of APP were also discovered. [Holtzman *et al.*, 2011] APP is located on chromosome 21, and people with Down's syndrome, trisomy 21, present AD like symptoms at an early age and have neuronal amyloid plaques. [Masters *et al.*, 1985] Both these observations have contributed to one of the main hypothesis about the neuropathology of AD, which propose that the primary event is the accumulation of Aβ. [Hardy and Selkoe, 2002]

1.2 Amyloid precursor protein (APP)

Aβ is as mentioned derived by proteolytic cleavage of APP [Zheng and Koo, 2011]. APP is a member of a family of type I transmembrane glycoproteins [Aydin *et al.*, 2011] which in mammals also include amyloid precursor-like protein 1 and 2 (APLP1 and APLP2, respectively). The latter two share sequence similarity with APP except the Aβ sequence is not conserved in these proteins, making this sequence unique to APP. They all have a large extracellular domain, one transmembrane region and a short cytoplasmic domain. The latter is designated the APP intracellular domain (AICD). [Zheng and Koo, 2011] The APP gene contains 18 exons, and different isoforms of the gene product exist. The splice variant APP695 is primarily expressed in neurons, whilst the two other major variants APP751 and APP770 are predominantly expressed in other cell types. The extracellular domain of APP contains E1 and E2 domains and a Kunitz protease inhibitor domain, which is missing in APP695. [Zhang *et al.*, 2012] APP is localized to different structures of the cell including the plasma membrane, endoplasmatic reticulum, Golgi bodies, endosmes, and lysosomes. [Guo *et al.*, 2012]

As illustrated in Figure 2, APP can be cleaved through two mutually exclusive pathways; the amyloidogenic pathway, and the non-amyloidogenic pathway. The amyloidogenic pathway involves first cleavage by the protease β-secretase, generating secreted amyloid precursor protein beta (sAPPβ) and with subsequent cleavage by a second protease, γ-secretase, Aβ of various lengths ($A\beta_{1\text{-}39,40,42,43}$) are generated, and the AICD is released into the cytosol. The non-amyloidogenic pathway involves cleavage of APP by another protease, α-secretase, generating the neuroprotective protein secreted amyloid precursor protein alpha (sAPPα) that has 16 extra amino acids at its C-terminal compared with sAPPβ. Additionally a membrane bound C-terminal fragment of 83 amino acids (C83) is produced. The membrane bound fragment can be further cleaved by γ-secretase, resulting in the secretion of the small peptide P3 and release of AICD. [Eggert *et al.*, 2009] In a normal functioning brain there is a fine balance between these two pathways, however a disruption in this balance is observed in patients with AD shifting the cleavage of APP towards the amyloidogenic pathway [Tyler *et al.*, 2002]. A decrease in sAPPα has been observed both in patients suffering of FAD and in people with sporadic AD [Sennvik *et al.*, 2000].

1.2.1 Function of APP

APP contributes to cell adhesion through its extracellular domains E1 and E2, which have been found to interact with extracellular matrix proteins like heparin and collagen. [Xue *et al.*, 2011; Beher *et al.*, 1996] In addition to this, these two regions E1 and E2 have also been found to be involved in the formation of a APP homodimer and APP/APLPs heterodimers. [Xue *et al.*, 2011; Soba *et al.*, 2005] The transmembrane domain of APP has also been reported to be involved in APP dimerization [Munter *et al.*, 2007]. The

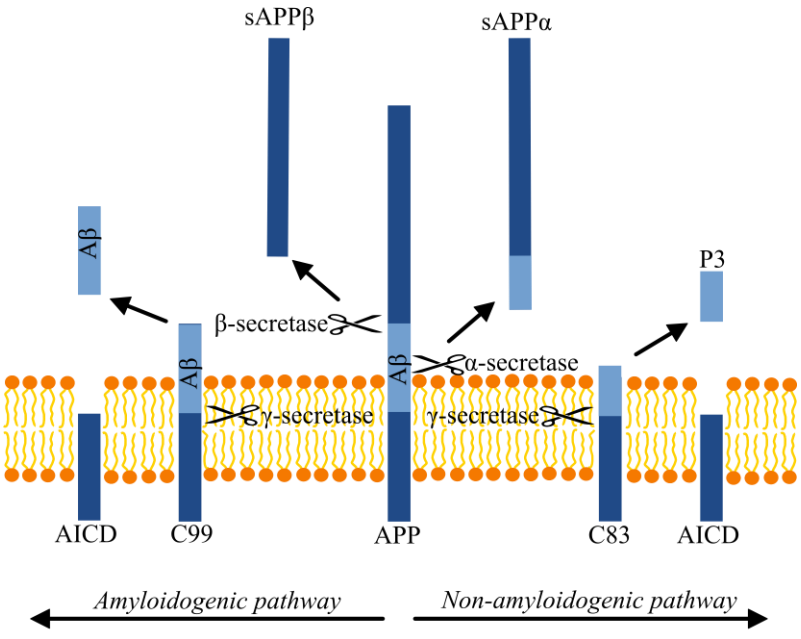

Figure 2: Illustration of the proteolytic cleavage of amyloid precursor protein (APP). *Left* side of the figure shows the amyloidogenic pathway involving cleavage of APP by β- and γ-secretase generating sAPPβ and Aβ. *Right* side of the figure shows the non-amyloidogenic pathway which involves cleavage of APP by α- and γ-secretase generating sAPPα and the small peptide P3.

interaction between APP and APLPs has been suggested to be both at the cell surface and intercellular contributing to cell to cell adhesion. [Soba *et al.*, 2005] Homodimeric APP has been associated with increased susceptibility with cell death [Shaked *et al.*, 2006; Gralle *et al.*, 2009]. APP heteromeric complexes with the APLPs [Soba *et al.*, 2005], and Notch receptors [Oh *et al.*, 2005] have been implicated in the regulation of neurite outgrowth and retraction [Libeu *et al.*, 2011].

APP has a highly similar structure with Notch and is therefore also suggested to function as a cell surface receptor. This has been supported by several studies, where APP has been implicated as the receptor for Aβ [Libeu *et al.*, 2011], sAPPα [Gralle *et al.*, 2009], Nogo-66 [Zhou *et al.*, 2011], netrin-1 [Lourenco *et al.*, 2009], and ApoE [Haas *et al.*, 1997]. The binding of these molecules result in modulation of APP processing and transmission of sequential downstream signals [Zheng and Koo, 2011].

1.3 Function of sAPPα and sAPPβ

The single difference between sAPPα and sAPPβ is the 16 extra amino acids at the C-terminus of sAPPα [Baratchi *et al.*, 2011]. These 16 amino acids are of special interest since they form the last part of the sAPPα as well as the first part of Aβ [Nunan and Small, 2000].

sAPPα has been found to be neuroprotective [Furukawa *et al.*, 1996], involved in normal memory function and in long term potentiation (LTP) [Taylor *et al.*, 2008], and have neurotrophic properties [Chasseigneaux *et al.*, 2011; Ninomiya *et al.*, 1993].

The effect of sAPPα on neurite outgrowth has been localized to two domains located between residues 96-110 and 319-335 of the molecule. Region 96-110 is also a binding site for heparan sulfate proteoglycan. [Chasseigneaux *et al.*, 2011] The five amino acids RERMS at position 328-332 of the 319-335 residues are the motif responsible for the growth promotion effect of sAPPα [Ninomiya *et al.*, 1993]. Furthermore, Mileusnic et al., 2005, reported that both the RERMS and the smaller peptide RER could rescue memory in animals rendered amnestic by antibody, antisense, and Aβ pretreatments. They suggest that this effect is mediated through a receptor. [Mileusnic *et al.*, 2005]

Neurotropic effects have been found to be mediated partly through activation of the MAPK/ERK pathway [Gakhar-Koppole *et al.*, 2008]. And Chasseigneaux *et al.*, 2011, discovered that the amount of Egr 1 increased in response to sAPPα and sAPPβ and the change is blocked by inhibiting ERK. They confirmed that both sAPPα and sAPPβ can induce axonal outgrowth, but sAPPα is much more potent than sAPPβ. [Chasseigneaux *et al.*, 2011] Young-Pearse *et al.*, 2008 showed that sAPPα cannot stimulate neurite outgrowth in the absence of cell surface APP, and that both might modulate their effect through binding with integrin β1. The binding was competitive in favor of sAPPα, suggesting that sAPPα regulates the ability of APP to suppress integrin β1 induced neurite outgrowth. When APP binds integrin β1, no neurite outgrowth was observed. However, by contrast when sAPPα bound, the neurite outgrowth was enhanced. [Young-Pearse *et al.*, 2008]

sAPPα is able to protect neurons against excitotoxicity [Furukawa *et al.*, 1996], Aβ toxicity [Goodman and Mattson, 1994], and glucose deprivation [Furukawa *et al.*, 1996; Turner *et al.*, 2007] up to 100-times more effective than sAPPβ. This has fur-

ther focused attention towards the 16 amino acids at sAPPα's C-terminus. Isolation of short sequences of sAPPα has lead to the discovery that the neuroprotective activity is localized to amino acids 591-612 at the C-terminus. The heparin binding domain –VHHQK- within this region has been found to be particularly effective at mediating the increased potency of sAPPα to protect neurons against ecxitotoxicity and Aβ toxicity, since the protective effect of sAPPα can be reduced by addition of heparinases. [Furukawa *et al.*, 1996] Another proposed mechanism by which sAPPα can protect against Aβ toxicity is by stabilizing calcium homeostasis and activate NF-κB to counteract the apoptotic effect of Aβ [Guo *et al.*, 1998]. sAPPα can also counteract the effect of Aβ by binding to β-secretase thereby preventing the formation of Aβ. It is suggested that sAPPα is involved in a positive feedback loop whereby it promotes its own production by blocking β-secretase activity. [Obregon *et al.*, 2012] Furthermore, sAPPα has also been found to protect neurons against iron induced neurotoxicity [Goodman and Mattson, 1994].

sAPPα can protect neuroblastoma cells against starvation induced cell death. This effect is suggested by Gralle *et al*. 2009 to involve binding of sAPPα to APP, since it was found that when the APP dimer is disrupted in response to sAPPα binding it promotes cell survival. It was suggested that sAPPα interact by a direct interaction model as illustrated in Figure 3A. [Gralle *et al.*, 2009] Moreover, sAPPα has been found to be neuroprotective against traumatic brain injury in rats, where administration of sAPPα following the brain injury resulted in improved motor function and reduction in the extent of axonal injury [Thornton *et al.*, 2006].

LTP has been shown to be enhanced in hippocampal slices in response to sAPPα [Ishida *et al.*, 1997] and in the dentate gyrus in response to intrahippocampal infusion of sAPPα [Taylor *et al.*, 2008]. These findings could explain some of the memory deficiency seen in AD since sAPPα is decreased in the AD brain, and thereby cannot contribute to LTP to the same extent as in the non-diseased brain [Taylor *et al.*, 2008].

1.4 Aβ

Aβ peptides are ~4 kDa polypeptides containing between 39 and 43 amino acid residues, with the main alloforms consisting of 40 and 42 amino acids [Gregory and Halliday, 2005]. Under non-pathological conditions Aβ is involved in various proposed functions. In a study by Giuffrida *et al.* 2009, monomeric $A\beta_{1-42}$ completely rescued neurons from tropic deprivation and protected mature neurons against excitotoxic death. The neuroprotective effect of Aβ was proposed to be through enhanced activity of the PI3K pathway, as increased phosphorylation of Akt was observed. [Giuffrida *et al.*, 2009] Monomeric Aβ has also been found to act as a natural antioxidant molecule that prevents neuronal death caused by transition metal-induced oxidative damage [Zou *et al.*, 2002]. Furthermore, Aβ has been implicated in synaptic regulation. The formation of Aβ is promoted in response to increased neuronal activity, and the increased Aβ formation depresses the synaptic function, thereby acting as a negativ feedback regulator. [Kamenetz *et al.*, 2003]

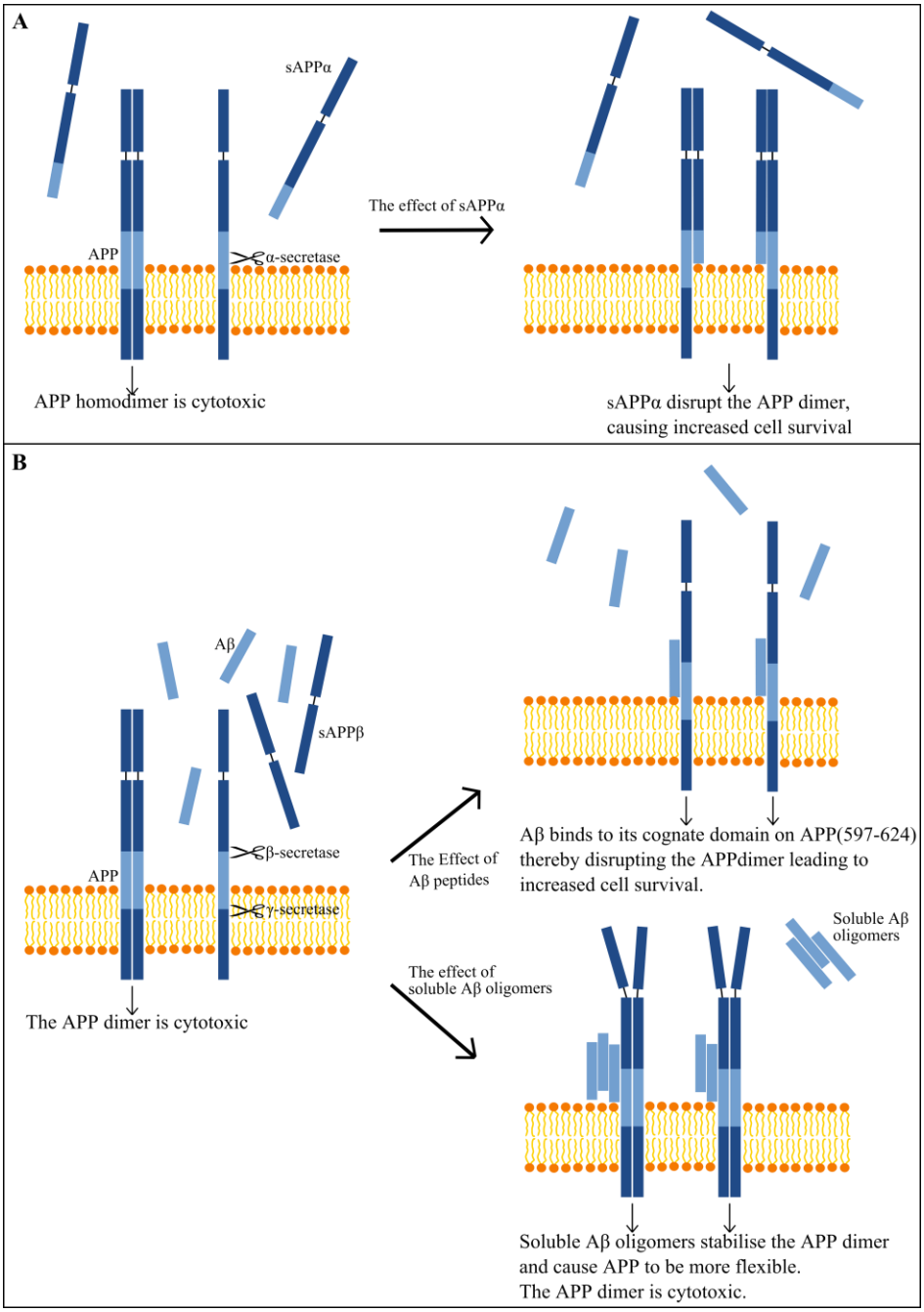

Figure 3: Illustration of the regulation of APP dimers by sAPPα and Aβ. **A**. The APP dimer is proposed to be cytotoxic and sAPPα can bind and disrupt the dimer, thereby promoting cell survival. **B.** Aβ peptide can also disrupt the APP dimer whereas soluble Aβ oligomers stabilize the dimer and causes APP to be more flexible.

However, Aβ is also proposed to be the primary neurotoxin in AD, and has been shown to modulate its effect through both chemical and physical effect on cells. [Libeu *et al.*, 2011] In AD, a change in the state of Aβ is observed. Aβ starts to form dimers, and higher oligomers that can aggregate further into fibrils. The soluble oligomers of $A\beta_{1\text{-}40}$, and the longer allo-form $A\beta_{1\text{-}42}$, are more amyloidogenic that the shorter monomeric $A\beta_{1\text{-}40}$ and the fibrillar forms of Aβ. [Marsden *et al.*, 2011] However, the reason for the changes in the form of Aβ among AD patients is still unknown. But both environmental and genetic factors have been implicated. [Jagust and Mormino, 2011]

APP has been found to regulate multiple functions through regulation of its dimeric, heterodimeric, or monomeric state, therefore attention has been drawn towards Aβ' signalling through APP. Shaked *et al.*, 2006, have shown that Aβ can induce cell death by interaction with dimeric APP through binding with its homologous region on APP (597-624) [Shaked *et al.*, 2006]. This has further been investigated by Libeu *et al.* 2011, who demonstrated that Aβ- monomers, and dimers disrupted APP dimers, promoting cell survival, and that only Aβ oligomers stabilise the APP dimer, see Figure 3B. When Aβ oligomers bound to APP, the extracellular domain became more flexible, and was suggested to enhance the probability of ligand interaction with APP. [Libeu *et al.*, 2011] The opposing effects of monomeric and oligomeric Aβ correspond well with the observation that monomeric Aβ is neuroprotective under non-pathological conditions, and that it is the larger soluble oligomeric forms of Aβ in the AD brain that stabilise the APP dimer and indce cell death.

The binding of Aβ oligomers to its cognate region on dimeric APP could possible interfere with α-secretase. This could explain some of the decrease in sAPPα observed in AD. [Libeu *et al.*, 2011] By contrast the amount of Aβ increases in response to disruption of APP dimers [Eggert *et al.*, 2009], indicating that the binding of Aβ to its cognate region interferes with the secretase activity. However, opposing results were reported by Scheuermann *et al.* in 2001 that dimerization of APP increased the production of Aβ. It is suggested that internalization of APP monomers would be less prone to Aβ production than internalization of APP dimers. [Scheuermann *et al.*, 2001]

2 Research aims

It is clear that APP and its secreted peptides: sAPPα, sAPPβ, and Aβ regulate multiple functions in the non-diseased brain and their function overlap. In AD the balance between the different proteins is disrupted.

sAPPα is much more potent at protecting neurons against various insults, inducing axonal growth, and in enhancing LTP, compared to sAPPβ, despite the only difference being the 16 amino acids at the C-terminus. These 16 amino acids, are also part of Aβ, the primary neurotoxin in AD.

The purpose of this study was therefore designated to investigate the relation between sAPPα and Aβ, asking the question:

- Does sAPPα interact with $A\beta_{1-42}$?

The aims of this study were therefore to:

1. Produce and purify recombinant Aβ and GST-tagged sAPPα, and GST-tagged sAPPβ
2. Investigate whether the proteins interact using a GST pull-down assay
3. If interaction is observed characterize the interaction site
4. Deduce the importance of such interactions to the aetiology of AD

3 Materials and Methods

3.1 Production of Aβ

3.1.1 Induction of MBP-Aβ production

A laboratory clone of $A\beta_{1-42}$ fused to a maltose binding protein carrier (MBP-$A\beta_{1-42}$), was seeded from a glycerol stock, into 5 mL Luria – Bertani (LB) medium (1 L: 10 g Peptone from casein, Merck, cat. no. 107213, 5 g yeast extract granulated, Merck cat. no. 103753, 10 g NaCl, AppliChem cat. no. A1149), with 0.5 mg ampicillin (Sigma-Aldrich cat. no. A9518-25G), and incubated overnight in the Innova 40 Benchtop incubator Shaker, 37 ˚C, shaking 200 rpm. This culture was added to 500 mL LB medium with 50 mg ampicillin and 0.01 M glucose (Scharlau cat. no. GL01271000) and grown until OD_{600nm} of 0.4-0.6 was reached. To induce the synthesis of MBP-$A\beta_{1-42}$, isopropylβ-D-1-thiogalac-topyra-noside (IPTG) (AppliChem, cat. no. A4773) was added to a final concentration of 1 mM, and the bacteria were grown for an additional 4 h. The bacteria were then harvested by centrifugating at 400×g using a JSP-F250 rotor for 15 min at 4 ˚C, the supernatant removed, and the pellet stored at -80˚C.

3.1.2 Lysis of the bacteria and extraction of crude protein fraction

The pellet was resuspended in 10 mL affinity chromatography buffer (20mM Tris-HCl, AppliChem cat. no. A1086, 0.2 M NaCl; pH 7.5). To crack open the bacteria, they were sonicated on ice with the Sonic Vibra Cell, 4 x 30 s bursts at 20KHz, 20% amplitude, and the mixture then centrifuged at 15000×g for 20 min at 4 ˚C in a JSP-F50C rotor. The supernatant, containing the protein was transferred to a 50 mL Falcon tube and subsequently applied to a 3 mL amylose resin column (NEB, cat. no. E8021L) in aliquots of 3 mL. The MBP tag effectively binds to the amylose resin which allows purification of MBP-$A\beta_{1-42}$. After incubating for 30 min at 4˚C, to allow binding of MBP-$A\beta_{1-42}$, the unbound proteins were washed of the column using affinity chromatography buffer and then the bound protein eluted using buffer containing maltose (20 mM Tris-HCl, 0.2 NaCl, 10 mM maltose, USB, cat. no. 18725; pH 7.5).

To concentrate the eluted protein ammonium sulphate (Scharlau, cat. no. Am04001000) was slowly added to the pooled elution fractions containing the protein to 60 % saturation (392 mg ammonium sulphate per mL). This was carried out at 4˚C over 30 min on a magnetic stirrer. After all the salt had been added the mixture was left for further 60 min with stirring.

To pellet the ammonium sulphate precipitated protein the slurry was centrifuged at 12000×g in a JA20 rotor for 30 min at 4 ˚C. The supernatant was carefully discarded and the pellet resuspended in either 2 mL 1 mM Tris-HCl buffer or 2 mL 20 mM Tris-HCl buffer pH 7.5.

3.1.3 Desalting chromatography

The MBP-$A\beta_{1-42}$ protein samples from the ammonium sulphate precipitation step were run through a HiTrap™ Desalting column (GE Healthcare, cat. no.17-1408-01) connected to an Akta™ Purifier Fast Protein Liquid Chromatography (FPLC) system to remove the salt, according to manufacturer's instructions. The absorbance of the protein was measured at 280nm, with elution in either 1 or 20 mM Tris-HCl in 1mL fractions. The protein-

containing fractions were collected and lyophilised overnight.

3.1.4 Reverse phase chromatography (RPC)

The dried samples were taken up in 50 µL of factor Xa protease cleavage buffer (20 mM Tris-HCl, 0.1 M NaCl, 2mM $CaCl_2 \cdot 2H_2O$; pH 8) for each mL of original solution and the protein concentration determined using a NanoDrop 1000 spectrometer, (Thermo Scientific). To cleave $A\beta_{1-42}$ from the carrier MBP 10 µg Factor Xa (NEB, cat. no. #P8010L) was added per mg of fusion protein and incubated for 16 h at 23 ˚C.

To separate $A\beta_{1-42}$ from the MBP, a Resource™ RPC column (GE Healthcare cat. no. 17-1181-01) connected to the Akta™ Purifier Fast Protein Liquid Chromatography (FPLC) system was used. The cleaved protein was mixed with buffer A (filtered ddH_2O with 5 % acetonitrile, 0.1 % trifluroacetic acid) and applied to the column and eluted at a flow rate of 1 mL/min running a gradient from 5-50 % (v/v) acetonitrile. The eluted protein was detected at an absorbance of 215 nm and the fractions containing protein were lyophilized, resuspended in 50 µL sterile ddH_2O, and analysed by SDS-PAGE and Western blotting.

3.1.5 Resolubilisation of Aβ

If Aβ aggregated during the production, it was resolubilised by addition of 10 mM NaOH, and sonicatated in a waterbath 10-20 min. Then to neutralise the solution five times the amount of NaOH of 0.1 M sodiumphosphate buffer (pH 7.4) was added. Then the solution was centrifuged 13000 rmp in Heraeus Pico 17 centrifuge (Thermo electron corporation) for 30 sec. If no pellet was observed, the solution was mixed with buffer A, and the proteins was ready to be applied to the Resource™ RPC column.

3.1.6 Determination of Aβ concentration

The fractions containing pure $A\beta_{1-42}$ protein were pooled and the concentration was determined using a Bicinchoninic Acid (BCA) Protein Assay Kit (Sigma, cat. no. BCA1, B9634), according to manufacturer's instructions. Bovine serum albumin (BSA) (Gibco, cat no. 30036-578) was used as a standard. The solutions were incubated at 60 ˚C for 20 min, before the absorbance at 562 nm was measured and the concentration of the protein calculated using the constructed BSA – standard curve. The BCA assay depends on the formation of Cu^+ from Cu^{2+}. This reaction is depended on cysteine, cystine, tryptophane, and tyrosine residues in the protein and at 60˚C the peptide bonds are also involved. BSA contains more interacting residues than $A\beta_{1-42}$, and an underestimate of the concentration of $A\beta_{1-42}$ is therefore expected when using BSA as standard. The concentration of Aβ can therefore be depicted as between $X_{\text{calculated conc.}}$ and 2 times $X_{\text{calculated conc.}}$. 1.5x $X_{\text{calculated conc}}$ was used to calculate amount of input protein in the pull-down assay.

3.2 Production of GST-sAPPα and GST-sAPPβ

3.2.1 Transformation

The strategy for the production of the GST-tagged proteins is illustrated in Figure 4. BL21 competent cells (100µl) were transformed with 20 ng pGEX-6P-3 vector DNA with insert of sAPPα or sAPPβ. Bacterial cells without any additional DNA were used as a control. The bacteria were left on ice for 15 min, heat shocked at 42

˚C for 45 s, and then kept on ice for further 1 min before 900 µL 2xYT medium (200 mL: 3.2 g peptone from casein, 2 g yeast extract granulated, 1 g NaCL) was added. Then the culture was incubated on the Innova 40 Benchtop incubator Shaker, 45 min at 37 ˚C, shaking at 200 rpm. Subsequently, 100 µL was plated on agar plates containing ampicillin and chloramphenicol (USB, cat. no. 2366025GM), and incubated overnight at 37 ˚C.

3.2.2 Induction and purification of GST-fusion proteins

A colony from each plate of the transformed bacteria was seeded in 10 mL LB medium containing 0.3 mg chloramphenicol and 1 mg ampicillin and grown over-

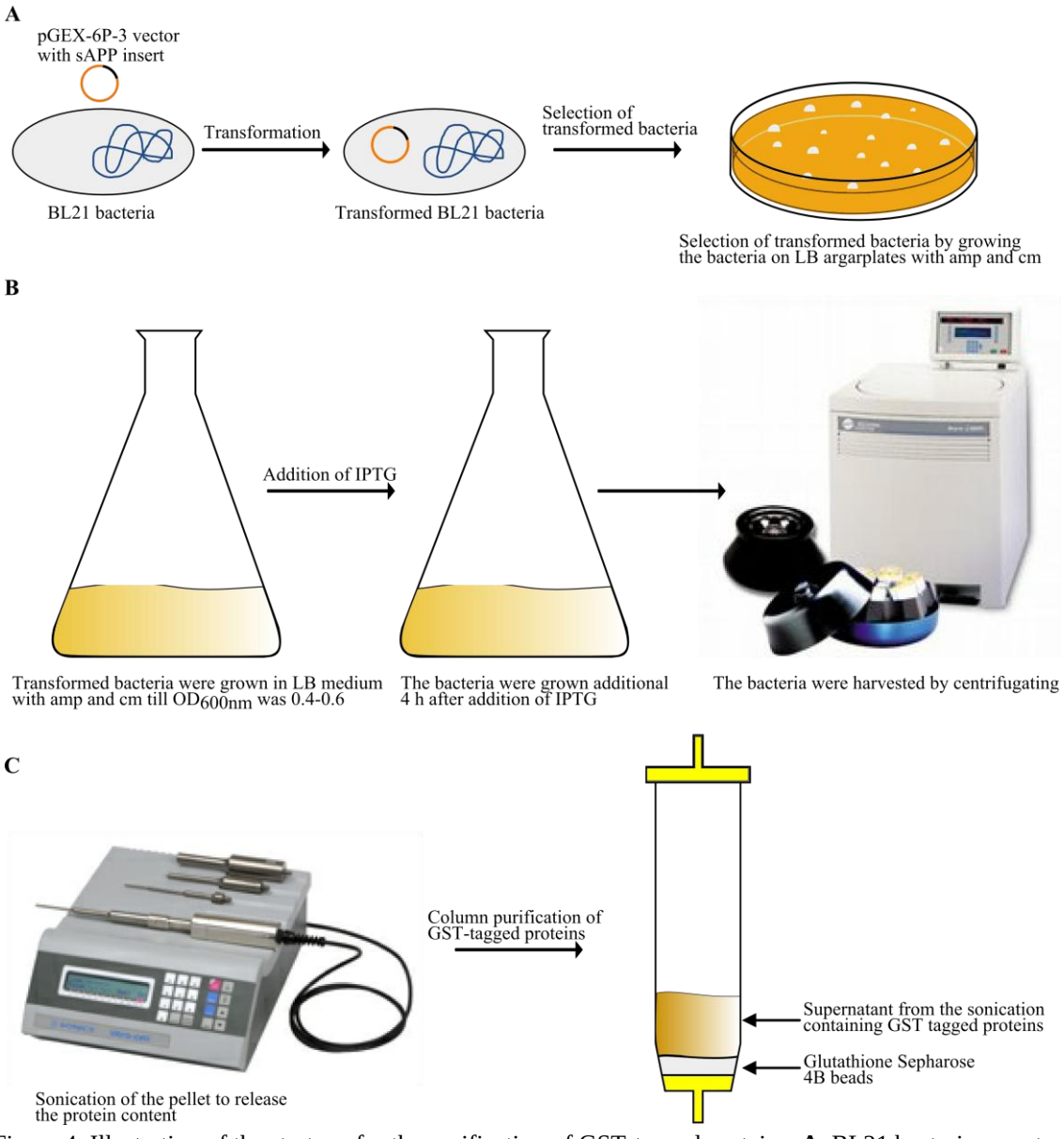

Figure 4: Illustration of the strategy for the purification of GST-tagged proteins. **A**. BL21 bacteria were transformed with pGEX-6P-3 vectors with sAPPα or sAPPβ inserts, and grown on LB argarplates with ampicillin (amp) and chloramphenicol (cm). **B.** Next a colony from the plate with transformed bacteria was grown in LB medium till OD_{600nm} was 0.4-0.6. To induce synthesis of the proteins IPTG was added and after 4 h of incubation the bacteria was harvested by centrifugation. **C**. The bacteria pellet was resuspended in sterile PBS, sonicated and applied to the column with Glutathione Sepharose 4B beads, whereby the GST-tagged proteins were purified.

night in the Innova 40 Benchtop incubator Shaker at 37˚C, shaking at 200 rpm.

The 10 mL cultures were then added to 500 mL LB medium with 50 mg ampicillin and 15 mg chloramphenicol and grown until OD_{600nm} was 0.4-0.6. IPTG 0.1 mM was added and the bacterial cultures were incubated for an additional 4 h at 25 ˚C, shaking at 200 rpm.

The bacteria were harvested by centrifugating at 4000 g in a JSP-F259 rotor for 10 min at 4 ˚C and the pellet was resuspended in 5 mL sterile PBS. Lyzozyme was added to a final concentration of 1 mg/mL and the bacteria lysed on ice by sonication with 10 x 10 sec bursts at 20KHz, and 30 % amplitude in order to break the bacteria open. The lysed bacteria were centrifuged at 12000×g in JA20 rotator for 10 min at 4 ˚C, and the supernatant was further clarified by recentrifugation. The supernatant, containing the proteins was applied to a column of 1.5 mL pre-swollen glutathione sepharose™ 4B beads (GE Healthcare, cat. no. 17-0756-01) and left overnight at 4˚C with gentle rotation. GST binds to the glutathione sepharose™ 4B beads which enables the purification of GST-tagged proteins. The column was washed with sterile PBS (x3) and bound protein eluted with elution buffer (10 mM glutathione in 50mM Tris-HCl; pH 8.0) in four 1 mL fractions, then the coulumn was left in 5 mL elution buffer overnight at 4 ˚C while rotating gently. The protein containing fractions were then dialysed 3 x 2 h in 1 L sterile PBS in order to remove the glutathione.

The protein concentration was determined by the mean of Qubit™ fluorometer (Invitrogen, cat. no. Q32857), in accordance with the manufacturer's instructions.

3.3 GST pull-down assay

In order to test if sAPPα or sAPPβ interacted with $Aβ_{1-42}$, a GST pull-down assay was performed. Figure 5 illustrates the strategy for the interaction assay. The GST tagged proteins are used as bait immobilised to glutathione sepharose™ 4B beads, and $Aβ_{1-42}$ added as prey.

Beads and GST was used as a control. First the binding condition for the GST-tagged proteins was tested at 4 ˚C overnight and 30 min at room temperature. Next the amount of input protein was tested to obtain maximal binding of GST-tagged proteins to the beads. Last the binding efficiency of the control GST was tested to standardize this to the amount of bound GST fusion proteins.

3.3.1 Testing of the binding conditions

To test the binding conditions for the GST fusion protein, 100 µg fusion protein was incubated with 20 µL of pre-swollen glutathione sepharose™ 4B beads for 30 min at room temperature or overnight at 4 ˚C. The samples were then centrifuged at 500×g for 5 min, washed 3 x in 100 µL PBS, and eluted with 2 x 40 µL elution solution. The samples were analysed with SDS-PAGE.

To test the amount of input protein, two concentrations (100 µg and 50 µg) of GST fusion protein was tested. The GST-fusion protein (50 µg or 100 µg) were incubated with glutathione sepharose™ 4B beads overnight at 4 ˚C and processed as described above.

3.3.2 Testing of binding efficiency of control GST protein

GST-fusion protein (100 µg) and GST (50 µg, 75 µg, and 100 µg) were incubated with 20 µL pre-swollen glutathione sepha-

rose™ 4B beads overnight at 4 ˚C, and processed as described above. The concentrations of proteins in flow through, wash 1, wash 2, and wash 3 were then measured using a Qubit™ fluorometer and subtracted from the input protein giving the approximate amount of protein bound.

3.3.3 Testing of interaction

GST-fusion protein (100 µg) or GST (20 µg) were incubated with preswollen glutathione sepharose™ 4B beads as described above. Then the beads were washed three times in PBS, washing off none bound GST-fusion protein, leaving GST-sAPPα and sAPPβ immobilised to the beads. The beads with immobilised bait were then incubated overnight at 4 ˚C with the prey in the following molar ratios, 1:1 sAPPα, 1:1 sAPPβ, and 1:5 $A\beta_{1-42}$. The non GST-tagged sAPPα and sAPPβ were provided from the research group [Turner *et al.*, 2007]. The samples were then centrifuged at 500×g for 5 min and washed three times in PBS before being eluted with 2 x 40 µL elution solution. The samples were then analysed by SDS-PAGE and Western blotting.

3.4 Characterisation of the interaction site between sAPPα and Aβ

In order to characterise the interaction site between sAPPα and $A\beta_{1-42}$, pGEX-6P-3 vectors with six variants of sAPPα were made. Figure 6 illustrates the different sAPPα variants. Vectors containing MBP-$A\beta_{1-16}$ and MBP-$A\beta_{17-42}$ were also constructed.

3.4.1 Production of pGEX-6P-3 vectors with sAPPα variants

pcDNA3.1D/V5-His-TOPO vectors containing the different sAPPα variants were

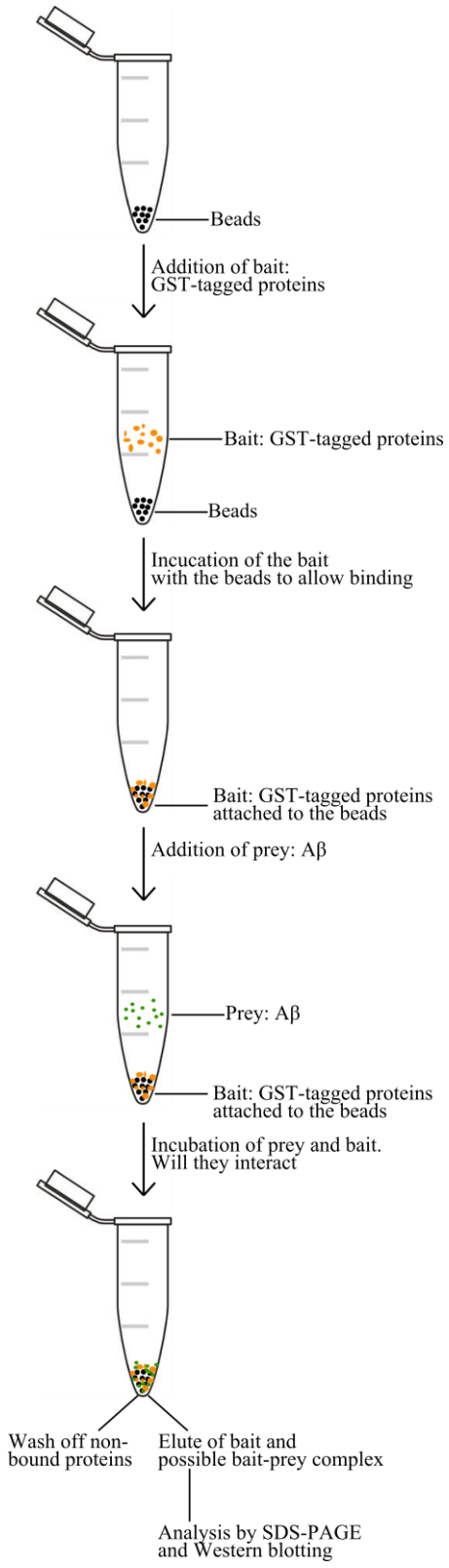

Figure 5: Strategy for the GST pull down assay. GST-tagged proteins were incubated with the beads, followed by the addition of the prey, Aβ. The mixture of bait and prey was incubated overnight to allow interaction. After incubation the non-bound proteins were washed of and bait and bait-prey complex eluted.

provided by the research group. To isolate the sAPPα variant fragments, the vectors were first digested with 4 U *Sma* I (Roche, cat no. 10220566001), for 2 h at 25˚C, and the fragments purified with the Qiagen QIAquick® PCR purification kit (cat. no. 28104) according to the manufacturer's instruction. The vectors were then further cut with 4 U *Not* I (Roche, cat no. 11014706001), for 2 h at 37˚C, and the samples were run on a 1.5 % (w/v) agarose gel at 90 v for 1 h. The 1.8 kb sized band corresponding to the sequence of each sAPPα variant was cut out and purified with the Qiagen QIAquick® Gel Extraction Kit (cat no. 28704) according to manufacturer's instructions. The pGEX-6P-3 vector was cut with the same enzymes and purified with the Qiagen QIAquick® PCR purification kit.

3.4.1.1 Ligation

In order to clone the sAPPα mutant sequences into the digested vector, 2 µL (10-50 ng) and 1.5 µL pGEX-6P-1 vector were mixed with 1 µL T4 DNA Ligase (Roche cat. no. 10481220001), 1 µL 10x Ligase buffer, and 4.5 µL sterile ssH_2O and incubated at 4 ˚C overnight.

To eliminate vectors not containing the mutated sAPPα inserts, 1 µL of the restriction enzyme 1 U *Sal* I (Roche, cat. no. 10348783001) was added and incubated for 1 h at 37 ˚C. Sal I only cuts empty vectors.

3.4.1.2 Transformation

DH5α bacteria (75 µL) were transformed with 6 µL vector as described in section 3.2.1, and plated on agar plates with LB and ampicillin.

3.4.1.3 PCR screening of colonies

From each plate of transformant, 5 colonies where screened by PCR to confirm that the colonies contain the vector with the sAPPα variant. Each colony was mixed with 6 µL LB medium, and 3 µL was transferred to 10 µL 0.5 % Tween-20. Then 1 µL of the Tween-20 was mixed with the PCR reaction mix containing:

- 1 µL Expand buffer
- 1 µL 2 nM dNTPs
- 0.075 µL Expand enzyme
- 0.2 µL 10 pmol/µl forward primer: pGEXfor
- 0.2 µL 10 pmol/µL reverse primer: APP933-1018rev
- 6.525 µL Sterile ddH_2O

The reaction was performed using the PTC-200 Peltier Thermal Cycler machine

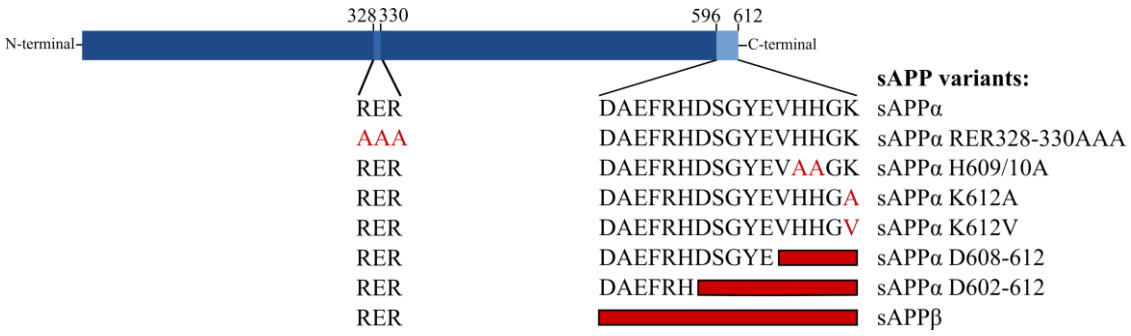

Figure 6: Overview of the different sAPPα variants. The red letters mark the change in sequence, and the red boxes the deletions.

running the following steps: firstly 95˚C for 5 min then 29 cycles (60˚C for 1 min, 72 ˚C for 1 min, 95 ˚C for 30 s) and finally 60 ˚C for 1 min; and 72˚C for 5 min.
The PCR samples were subsequently analysed on a 1.5 % (w/v) agarose gel. The positive colonies according to the PCR, were streaked on a masterplate and seeded in 5 mL LB medium with 5 µL ampicillin and kept overnight on the Innova 40 Benchtop incubator Shaker, 37 ˚C, shaking at 200 rpm.

3.4.1.4 Vector purification

Each transformed bacterial preparation was centrifuged at 13000 rpm in a Heraeus Pico 17 centrifuge (Thermo electron corporation) for 1 min, in fractions of 1 mL. Then the plasmids were purified using the Qiagen QIAprep® Spin Miniprep Kit (cat. no. 27106), according to manufacturer's instructions.

3.4.1.5 Digest screening of the purified vectors

To further confirm that the purified plasmids contained the sAPPα variants, the vector were cut with 1 U *EcoR* I and 1 U *Bgl* II for 2 h at 37 ˚C, and analysed on a 1 % (w/v) agarose gel. If there were two bands of 5 kb and 1.7 kb, respectively the vector was considered positive for having the insert and DNA was sent away for sequencing.

3.4.1.6 Analysis of sequencing results

The sequencing results were analysed by mean of BLASTn and BLASTx (NCBI). In the case of a base substitution, the sequence was also analysed by ExPASy Translate tool (http://web.expasy.org/translate/), in order to check if it would change the amino acid at that position. When sequences contained no errors, the clone was selected and the induction and purification method in section 3.2 was followed.

3.4.2 Production of $A\beta_{1-16}$ and $A\beta_{17-42}$

The plasmid containing $A\beta_{1-42}$ was purified with the Qiagen QIAprep® Spin Miniprep Kit and used for template for production of $A\beta_{1-16}$ and $A\beta_{17-42}$.

3.4.2.1 Primer design

The forward primers amplifying $A\beta_{1-16}$ and $A\beta_{17-42}$ where designed to contain an *Xba* I recognition sequence, a Factor Xa protease recognition sequence and a stuffer sequence at the 5' terminus. The reverse primers amplifying $A\beta_{1-16}$ and $A\beta_{17-42}$ were designed to contain a *Pst* I recognition sequence, a stop codon, and a stuffer sequence at the 3' terminus. The primers are shown in Table 1. The sequence for $A\beta_{1-42}$

Table 1: DNA primer sequences and annealing temperatures. The green letters correspond to the annealing sequence in Aβ, red the recognition site for the restriction enzyme, and blue the factor Xa protease recognition sequence.

Primer:	***Sequence:***	***Annealing temperature:***
Forward $A\beta_{1-16}$	5'-GTACGCTCTAGAATTGAAGGCCGTGATGCAGAATTCCGACATGAC-'3	58˚C
Reverse $A\beta_{1-16}$	3'-TAGTCCACTGCAGAAAGAACACCTATTTTTGATGATA-5'	58˚C
Forward $A\beta_{17-42}$	5'-GTACGCTCTAGAATTGAAGGCCGTTTGGTGTTCTTTGCAGAAGATG-3'	58˚C
Reverse $A\beta_{17-42}$	3'- GCTGTTCTGCAGTCACGCTATGACAACACCGCC-5'	58˚C

was found using the GenBank at NCBI and the designed primers were tested for primer-dimer and melting temperature using NetPrimer (© 2009 by PREMIER Biosoft International). An *in silico* PCR was performed using Amplify3 version 3.1.4 (© 2004, 2005, Bill Engels, University of Wisconsin), to ensure amplification of the correct product.

3.4.2.2 PCR amplification of $A\beta_{1-16}$ and A_{17-42} gene fragments

Each PCR reaction of 50 µL contained 0.2 mM dNTPs, 2 mM $MgSO_4$, 1X high fidelity PCR buffer, 1 U Platinum® *Tag* High Fidelity polymerase, 20 pmol forward primer, 20 pmol reverse primer, 10 ng DNA template, and ddH_2O. The reaction was performed using the PTC-200 Peltier Thermal Cycler machine running the following steps: first 95˚C for 4 min then 30 cycles (58 ˚C for 1 min, 72 ˚C for 1 min, 95 ˚C for 30 s.) and finally 58 ˚C for 1 min and 72 ˚C for 5 min.

After PCR amplification the product was purified using the QIAquick PCR purification kit, according to the manufacturer's instructions, and the concentration determined using the NanoDrop 1000 spectrometer (Thermo Scientific).

3.4.2.3 Restriction endonuclease digestion

To be able to ligate $A\beta_{1-16}$ and $A\beta_{17-42}$ into a pMAL-c2 vector, both the Aβ fragments and the pMAL-c2 vector were cut with 4U of each of the restriction enzymes *Xba* I (Roche, cat. no. 10674257001) and *Pst* I (Roche, cat. no. 10621625001) in a reaction of 40 µL containing 1X Roche buffer H. The digests were carried out for 2 h at 37 ˚C.

After the digestion the products were purified with the QIAquick PCR purification kit, according to the manufacturer's instructions, and the yield of DNA was determined using the NanoDrop 1000 spectrometer.

3.4.2.4 Ligation

Digested $A\beta_{1-16}$ or $A\beta_{17-42}$ and pMAL-c2 vector were ligated in a 10 µL reaction containing ~1:4 molar ratio of vector:insert, 1X T4 DNA ligase reaction buffer, and 1 U T4 DNA ligase. The ligation was carried out at 4 ˚C overnight.

3.4.2.5 Transformation

DH5α bacteria (75 µL) were transformed with 6 µL ligation mixture as described in section 3.2.1, and plated on agar plates with LB and ampicillin.

3.4.2.6 PCR screening and vector purification

From each plate, 6 colonies were screened by PCR as described in section 3.4.1.3. The primers used are listed in Table 1.

Plasmids from positive colonies were purified as described in section 3.4.1.4.

3.4.2.7 Digest screening of the purified vectors

To further confirm that the vectors contained the inserts of $A\beta_{1-16}$ and $A\beta_{17-42}$, they were cut with *Xba* I and *Pst* I as described in section 3.4.2.3, and the products fractionated on a 1 % (w/v) agarose gel. If there were two bands the clone was considered positive for having the insert and vector DNA was sent away for sequencing to confirm this.

The sequencing results were analysed as described in section 3.4.1.6. For clones containing sequences with no errors, the induction and purification method in section 3.1 was followed.

3.5 Agarose gel electrophoresis

The DNA samples analysed by agarose gel electrophores (PCR and plasmid samples) were mixed with 1x loading buffer and fractionated on either a 1 % (w/v) or 1.5 % (w/v) gel in 0.5 x TBE buffer, at 90V or 100V respectively. The gels were run 1h and DNA observed under UV light. Pictures were taken using a Gel Doc gel imager (BioRad, USA)

3.6 Sodium Dodecyl Sulfate-Polyacrylamide Gel Electrophoresis (SDS-PAGE)

Protein samples were analysed by SDS-PAGE. The gels were made from the following buffers: 4x separating gel (250 mL: 10 mL 10% SDS, 90.86 g Tris-Hcl, pH 8.8), 4x stacking gel (200 mL: 8 ml 10 % SDS, 12.114 g Tris-HCl, pH 6.8), 30% Acrylamide/Bis solution (BioRad, cat. no. #161-0154), 10 % ammonium persulphate solution, and Tetramethylethyl-enediamine (TEMED) (BioRad, cat. no.#161-0800).

GST tagged proteins, and MBP fusion proteins were analysed on a 10 % separating gel. The gels were loaded with samples and a broad range SDS-PAGE marker (BioRad, cat. no. 161-0317). The proteins were separated by electrophoresis at 200V for 80 min using a BioRad PowerPac 300.

$A\beta_{1-42}$, $A\beta_{1-16}$, and $A\beta_{17-42}$ were fractionated on a 16 % separating gel. The gels were loaded with samples and polypeptide SDS-PAGE standards (BioRad, cat. no. 161-0317). The proteins were separated by electrophoresis at 96V for 7 min, followed by 110V for 85 min using a BioRad PowerPac 300.

3.6.1 Coomassie Blue R-250 staining

After electrophoresis the gels were stained in Coomassie Blue R-250 (100 mL: 0.25 g Brilliant Blue R-250, 45 mL MeOH, 45 mL H_2O, 10 mL Glacial Acetic acid) for 1 h with shaking, and background stain removed with destain (1 L: 50 mL MeOH, 75 mL Acetic acid, 875 ml ddH_2O). After 1 h, the destaining solution was changed and the gel left overnight with shaking.

3.7 Western blotting

GST tagged proteins separated by SDS-PAGE were electroblotted onto a Protran® nitrocellulose membrane (Whatman cat no. 10401196). The electrophoretic transfer was carried out for 1 h, at 100V.

$A\beta_{1-42}$, $A\beta_{1-16}$, and $A\beta_{17-42}$ proteins separated by SDS-PAGE were electroblotted onto an Amersham-Hybond™-P hydrophobic polyvinylidene difluoride (PVDF) membrane (GE Healthcare cat. no. RPN2020F), which had been pretreated for 30 s in MeOH, rinsed in water, and left for 2 min in transfer buffer. The electrophoretic transfer was carried out for 1 h, at 28V.

Both transfers were carried out in transfer buffer (1 L: 3.03 g Tris, 14.4 g Glycine,

Table 2: Overview of the different primary and secondary antibodies used for Western blotting.

Antibody:	***Raised in:***	***Dilution:***	***Cat. no.***
Anti-Aβ 4G8	Mouse	1:1000	Covance: SIG-39220
Anti-Aβ 6E10	Mouse	1:1000	Covance: SIG-39320
Anti-GST	Goat	1:10000	GE Healthcare: 27-457701
Anti-N-terminus APP	Rabbit	1:10000	Sigma-Aldrich: A8967
α-mouse HRP conjugate	Goat	1:1000	Sigma-Aldrich: A9917
α-rabbit HRP conjugate	Goat	1:10000	Pierce: 32460
α-goat HRP conjugate	Rabbit	1:10000	Sigma-Aldrich: A5420

200mL MeOH) and kept cold by an ice container and stirring. After transferring the proteins to the membrane, the membrane was stained with Ponceau stain in order to identify and mark the markers.

The membrane was then blocked overnight at 4 ˚C in 1x PBS-Tween-20 with 1 % or 5 % (w/v) milk powder with shaking, incubated with primary antibody in 1x PBS-Tween-20 with 1 % milk powder for 2 h at room temperature, and washed three times of 10 min in 1x PBS-Tween-20. Then the secondary HRP-conjugated antibody diluted in 1x PBS-Tween-20 was applied for 1 h at room temperature. The membrane was then washed three times of 10 min with 1x PBS-Tween-20 and the proteins detected with enhanced chemiluminescence (ECL) Western blotting detection reagent (GE Healthcare, cat. no. RPN2106), according to manufacturer's instructions. An overview of the different primary and secondary antibodies can be seen in Table 2.

The chemiluminescence on the membrane was developed using a Fujifilm Las-3000.

3.7.1 Analysis of Western blot results

The relative amount of bound protein in the interaction assays was determined with densitometry using the programme ImageQuant TL. For each analysis the background was subtracted, and the intensity of each band was normalized to the sum of the total intensity of the bands in the flow through, washes, and eluted protein fractions.

3.8 Statistic Analysis

Bar charts of the interaction assays are expressed as mean ± SEM. For statistical analysis, the data was first tested for normal distribution by mean of a Shapiro-Wilk test and then analysed by an independent sample t-test using PASW statistics 18 (IBM Compan, Inc.). $P < 0.05$ was considered as statistically significant.

In the case of an outlier in the results, a Grubbs' test was performed. A Grubbs' test tests if the value is a significant outlier from the rest [Grubbs, 1969].

4 Results

The strategy for the production of the GST fusion proteins is illustrated in Figure 5, Materials and Methods. Firstly the bacteria were transformed with pGEX-6P-3 vectors containing sAPPα or sAPPβ inserts, then grown overnight in LB medium, before being further diluted in LB. IPTG was used to induce gene expression from the vector and initiate sAPP-protein production. After a further 4 h post induction the bacteria were harvested, and the GST tagged sAPP-proteins purified using glutathione Sepharose 4B beads.

4.1 Production of GST-tagged sAPPα and sAPPβ

GST tagged sAPPα and sAPPβ proteins were successfully synthesised in the bacteria after adding IPTG, see, lanes 2 and 4 (~116 kDa) Figure 7A. The identities of the proteins were confirmed on a Western blot, using the antibody to the N-terminus of APP, see Figure 7B.

In order to purify the proteins they were mixed with glutathione Sepharose 4B beads. Figure 8 illustrates the purification of the sAPPα fusion protein. The first lane contains a sample of the unbound flow through proteins (FT), an overloaded large

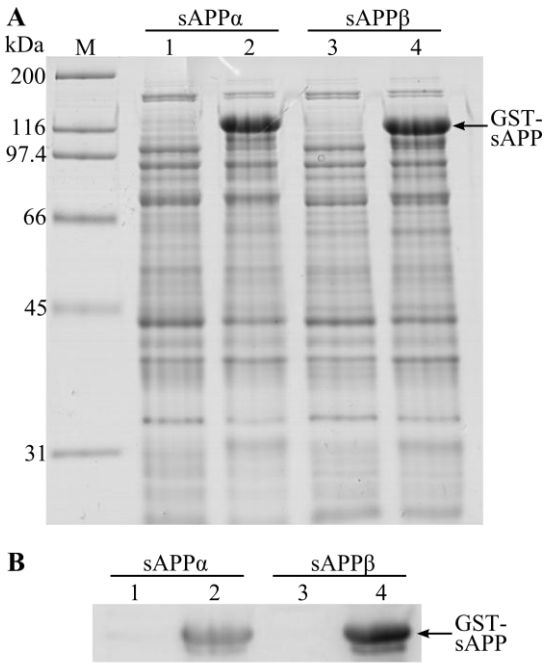

Figure 7: **A**. SDS-PAGE gel illustrating uninduced and induced samples of GST tagged sAPPα and sAPPβ in BL21 bacteria. **B**. Western blotting (WB), anti-N-terminal APP to confirm the identity of the protein. M: Broad range marker, 1 and 3: Uninduced samples, 2 and 4: Induced samples.

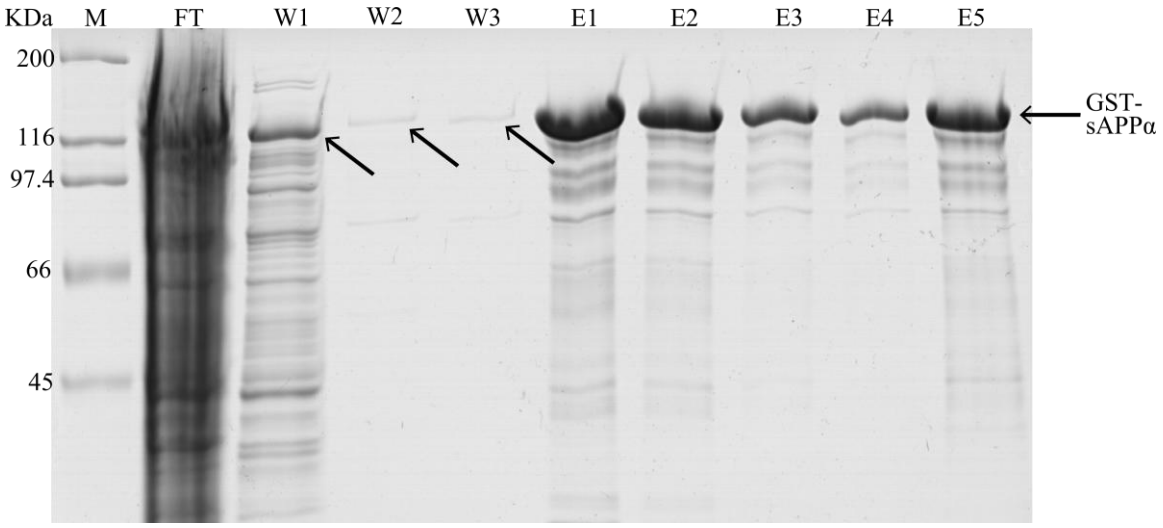

Figure 8: SDS-PAGE gel illustrating the purification of GST-sAPPα. M: Broad range marker, FT: Flow through after sonication, W: Wash with PBS, E1-E4: Eluted protein, after 10 min incubation. E5: Overnight eluted protein fraction. The angled arrows point at GST-sAPPα present in the washes.

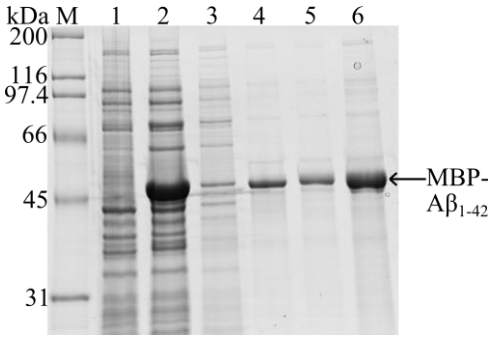

Figure 9: SDS-PAGE gel illustrating production and purification of $A\beta_{1-42}$. M: Broad range marker, 1: Uninduced, 2: Induced, 3: Flow through, 4: Elute, 5: After ammonium sulphate precipitation, 1mM Tris-HCl, 6: After ammonium sulphate precifitation, 20 mM Tris-HCl.

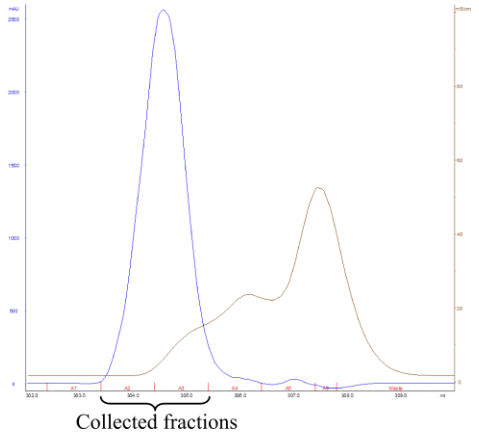

Figure 10: A graph illustration the desalting profile of the MBP-Aβ protein. The blue trace illustrates the proteins absorbed at 280 nm, and the brown trace is the conductivity which represents the salt elution. The collected fractions are illustrated by the bracket.

smear of proteins. Then any remaining unbound proteins were washed off (W1-W3). A fraction of GST-sAPPα did not bind to the beads and was present in the flow through and washings, as indicated by the angled arrows. The bound GST-sAPPα was eluted in five fractions see Figure 8 E1-E5, E5 represents the eluted protein fraction after overnight incubation. The purification of sAPPβ had the same profile (data not shown).

After purification the concentrations of each protein was determined. The cultures gave a yield of 4-6 mg of purified protein per 0.5 L.

4.2 Production of $A\beta_{1-42}$

A glycerol stock containing bacteria with pMAL-c2 vectors with $A\beta_{1-42}$ was provided by the research group. The bacteria were grown in LB medium with ampicillin and glucose, and after induction with IPTG the MBP tagged $A\beta_{1-42}$ was successfully expressed, see Figure 9 lane 2 (~45 kDa). MBP-$A\beta_{1-42}$ was purified on an amylose resin column, a small amount was present in flow through, see lane 3 (~45 kDa) Figure 9, but the majority of protein was present in the eluted fraction, lane 4 (~45 kDa).

The eluted protein was concentrated by ammonium sulphate precipitation, and re-suspended in either 1 mM or 20 mM Tris-HCl, see Figure 9 lanes 5 and 6 (~45 kDa). To remove the salt, a desalting column was used. Aliquots of 0.5 mL were loaded and the fraction containing the MBP-$A\beta_{1-42}$ protein collected, shown with a bracket on Figure 10.

The next step was to remove the carrier MBP using factor Xa protease cleavage overnight at 23 ˚C. This has previously been shown to be the most optimal condition for the cleavage. Figure 11 illustrates

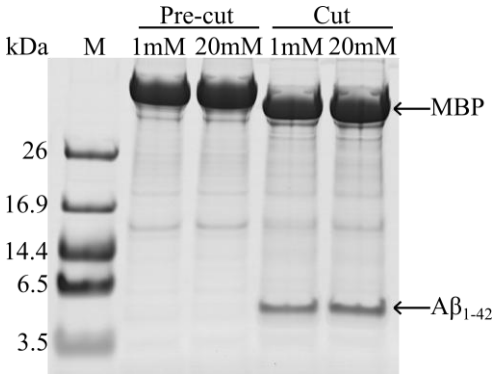

Figure 11: SDS-PAGE gel illustrating the cleavage of the carrier MBP from Aβ at two Tris-HCl concentrations. M: Peptide marker.

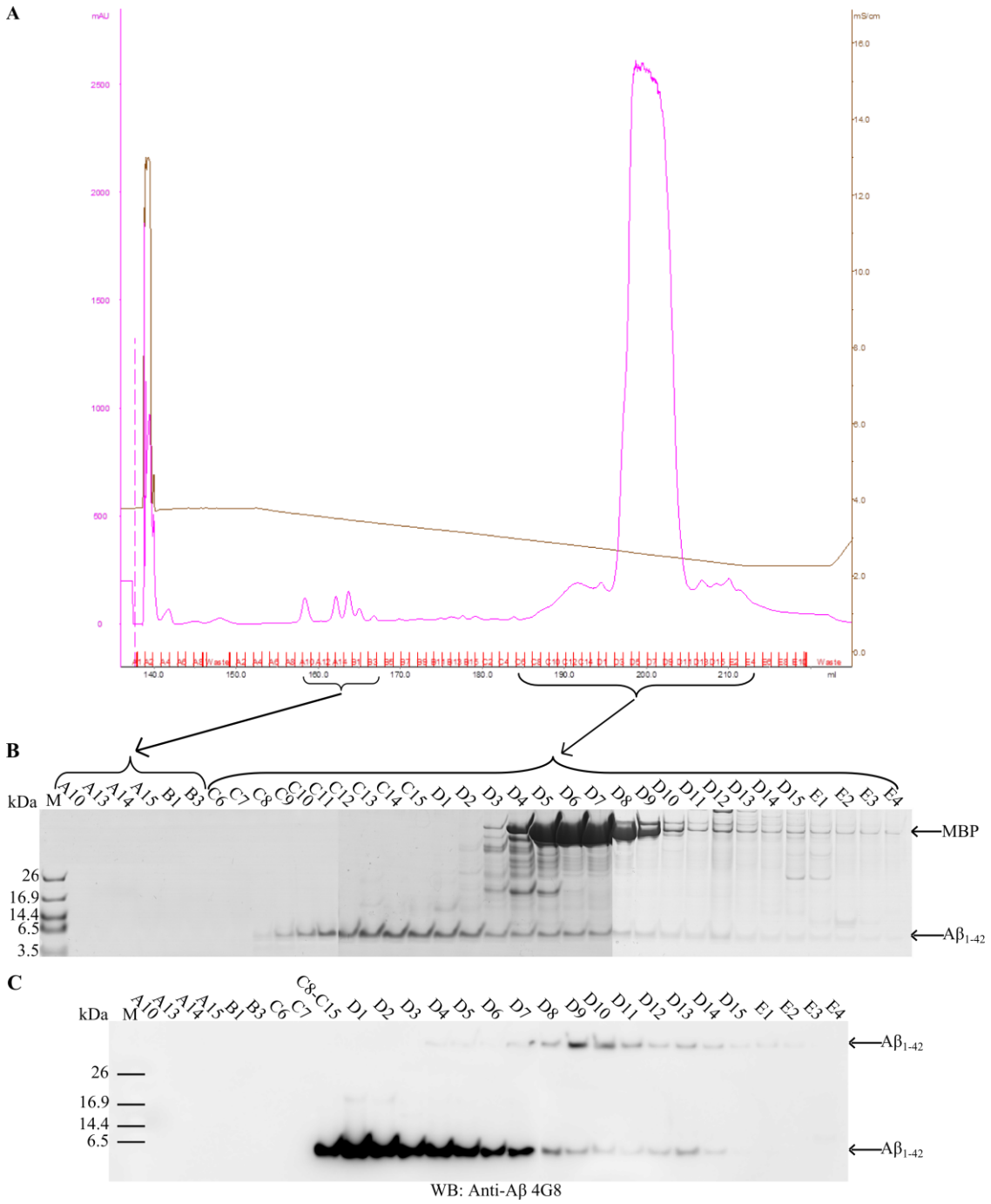

Figure 12: **A**: Fractionation of MBP and $A\beta_{1-42}$ on RPC. The pink trace illustrates the proteins absorbed at 215 nm, and the brown trace is the conductivity which represents the change from 5-50 % acetonitrile of the buffer. **B**: SDS-PAGE gel analysis of the fractions containing protein, marked by the two brackets. Fraction C8-C15 contains pure Aβ protein and is therefore pooled**. C**: Western blotting with the anti-Aβ antibody 4G8 to confirm the identity of the protein. Lane D4-E2 contains uncleaved fusion protein. M: Peptide marker.

the cleavage of the carrier MBP from $A\beta_{1-42}$, with a shift of the relative mass weight of the uncut MBP $A\beta_{1-42}$ following cleavage.

To isolate $A\beta_{1-42}$, a RPC column was used running a gradient of 5-50 % (v/v) acetonitrile. The protein was detected at wavelength 215 nm, which measures the peptide bonds. The fractions containing protein,

shown by the brackets on Figure 12A, were analysed with SDS-PAGE and Western blotting with the antibody 4G8 directed against amino acids 17-24 of Aβ, see Figure 12B and C, respectively. A minor fraction of $A\beta_{1-42}$ had not been cleaved from the MBP, and can be seen in fraction D4-E2 (>26 kDa) Figure 12C. Fractions C8-C15 contain pure $A\beta_{1-42}$, as illustrated on Figure 12B, these fractions were therefore pooled and the protein concentration was determined using a BCA assay. The concentration was found to be 0.197 mg/mL for the batch of $A\beta_{1-42}$ that had been resuspended in 1 mM Tris-HCl, and 0.213 mg/mL for the one resuspended in 20 mM Tris-HCl. Two buffer concentrations were used in case of inhibition of cleavage of $A\beta_{1-42}$ from MBP. No difference was observed between samples kept in 1 and 20 mM Tris-HCl buffers.

4.3 GST pull-down assay

Before performing the GST pull-down assay investigating if sAPPα and $A\beta_{1-42}$ would interact, the optimal conditions for binding of GST-tagged proteins to the beads was investigated and an evaluation of the amount of protein that would bind was completed.

The amount of bound control GST was compared to the amount of bound GST-tagged protein.

4.3.1 Testing of experimental conditions

To test the binding of the GST-tagged proteins to the glutathione sepharose 4B beads, two conditions were chosen; 30 min at room temperature and overnight at 4 ˚C. As seen on the SDS-PAGE gel, Figure 13A, the greatest amount of bound GST-tagged protein was observed in the eluted

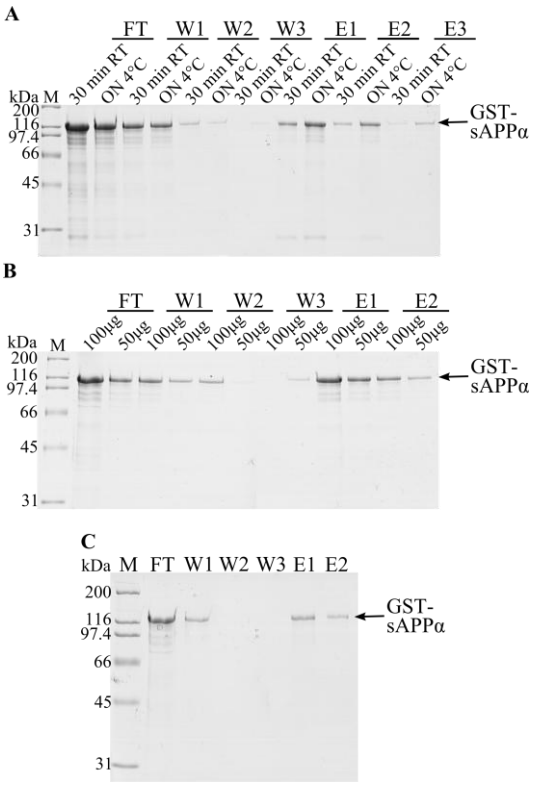

Figure 13: **A**. SDS-PAGE gel illustrating the binding of GST-sAPPα to glutathione sepharose beads after 30 min at room temperature (RT) and 4 ˚C overnight (ON), **B**. SDS-PAGE gel illustrating the binding of 100 µg and 50 µg GST tagged protein at 4 ˚C ON. **C**. Rebinding of the flow through from the pull down assay, showing that a fraction of GST-tagged protein cannot bind to the beads. M: Broad range marker, FT: Flow through, W: Wash, E1-E2: Eluted protein fraction, E3: Overnight eluted protein fraction.

protein fraction E1-E3 after incubating the GST-protein with beads overnight at 4 ˚C. Next, the amount of input protein was tested, and the amount of protein bound was greater when 100 µg GST-tagged protein was used, see the eluted protein fractions E1-E2 on Figure 13B.

As seen in both Figure 13A and B, a fraction of the GST-tagged proteins did not bind to the beads, and were present in the flow through (FT) and washes (W1-W3). In order to test if this were due to saturation of the beads, or if some of the proteins had folded in a way that they did not bind, the flow through was rebound to new beads. Only a small fraction of the origi-

nally unbound GST-tagged proteins now bound to the beads and was eluted, see the eluted protein fractions E1-E2 Figure 13C. The remaining protein was again found in the flow through and washes. This indicated that a fraction of the proteins did not bind to the beads.

As a control for the experiment, GST was used. In order to standardise the amount of control and test proteins bound to the beads, an input of 100 µg of GST-tagged proteins, was compared with 50 µg, 75 µg, and 100 µg of control GST. The concentration of the protein in the flow through and washes was then measured and subtracted from the input protein giving the approximate amount of protein bound. With an input of 100 µg GST tagged protein ~41 µg bound to the beads. To obtain the equivalent amount of bound control GST an input of 75 µg was needed. The amount of GST-tagged protein was standardised with the input of GST by standardising to equivalent molar concentrations.

4.3.2 Testing of interaction

On the basis of the results from optimising the experimental conditions, the pull-down assays were carried out with an input of 100 µg bait, GST-tagged protein, with binding overnight at 4 ˚C. Subsequently the prey sAPPα, sAPPβ, or $Aβ_{1-42}$ was applied and left overnight at 4˚C to allow interaction.

Firstly, GST-sAPPα was used as bait and untagged sAPPα and sAPPβ as prey. Figure 14 illustrates the results of the GST pull-down assays. The prey sAPPα and sAPPβ were present in the flow through (FT) as indicated by the arrow on Figure 14A and B (~97.4 kDa). No untagged sAPPα or sAPPβ was present in the eluted fractions E1 and E2 Figure 14. This indicated there was no apparent interaction between GST-sAPPα and sAPPα or sAPPβ. The reverse setup with GST-sAPPβ as bait and untagged sAPPα and sAPPβ as prey was also tested. This showed the same result (data not shown). To test if sAPPα and $Aβ_{1-42}$ interact, the pull-down assay was repeated with GST-sAPPα and GST-sAPPβ as bait and $Aβ_{1-42}$ as prey. The pull-down assay was repeated seven times, see Figure 15 for the results of experiment 1-3 and for the remainder Appendix I. Figure 15 illustrates the immunoblot analysis from experiments 1-3 with the anti-Aβ antibody 4G8. The immunoblots indicated a high degree of binding between sAPPα and $Aβ_{1-42,}$ much more than between sAPPβ and $Aβ_{1-42}$, as indicated by the asterisk at the eluted fractions (E1-E2) that contain $Aβ_{1-42}$ (<6.5 kDa).

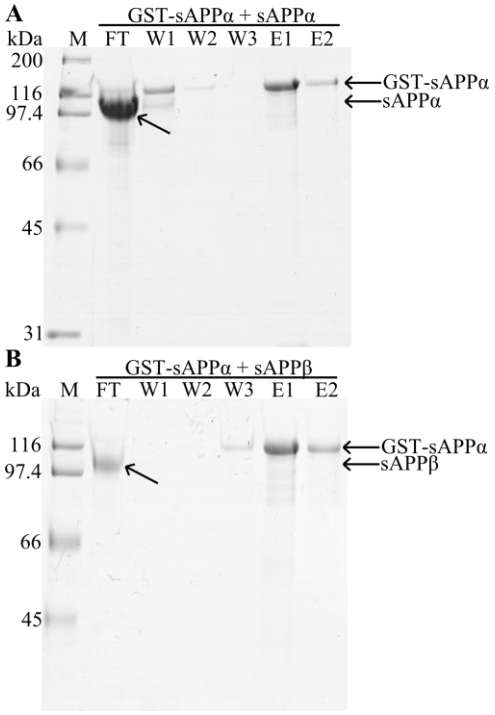

Figure 14: SDS-PAGE gels of the interaction assay with (**A**) GST-sAPPα and sAPPα and (**B**) GST-sAPPα and sAPPβ. M: Broad range marker, FT: Flow through, W: Wash, E: Eluted protein. The angled arrows mark the sAPPα and sAPPβ present in the flow through.

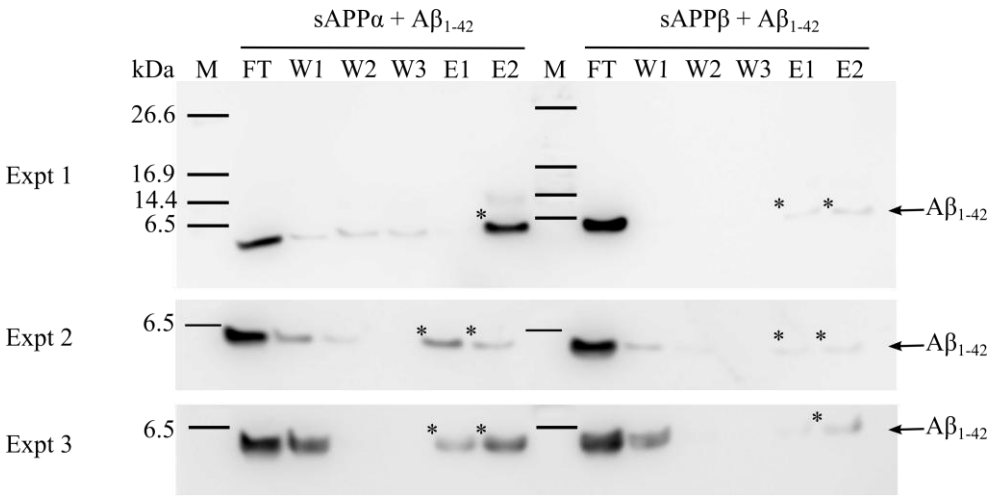

Figure 15: Western blotting with the anti-Aβ antibody 4G8 of three representative pull down experiments (Expt 1, 2, and 3), using sAPPα and sAPPβ as bait and $A\beta_{1-42}$ as prey. The *left* side illustrate the assays with sAPPα as bait, and the *right* side sAPPβ as bait. The asterisks indicate bound $A\beta_{1-42}$ showing much more $A\beta_{1-42}$ is bound to sAPPα than to sAPPβ. Expt: Experiment, M. Peptide marker, FT: Flow through, W: Wash, E: Eluted protein fractions.

One analysis (experiment 4, Appendix I) displayed strong binding of both sAPPα and sAPPβ to $A\beta_{1-42}$. The densitometry analysis of the Western blot result and subsequent Grubbs' test revealed the interaction between sAPPβ and $A\beta_{1-42}$ in experiment 4 as an outlier ($P < 0.05$). The result for both sAPPα and sAPPβ in this test was therefore excluded in subsequent analysis.

The results from the densitometry analysis of the Western blots from experiments 1-3, Figure 15, and 5-7, Appendix I, are presented in Figure 16 as a bar chart. sAPPα binds ~5 fold more $A\beta_{1-42}$ compared to sAPPβ. This difference is statistically significant ($P < 0.05$).

In order to test for unspecific binding of $A\beta_{1-42}$, the pull-down assay was repeated with beads and GST as bait. As indicated by the asterisks on Figure 17 no binding to the beads or GST was observed.

Since sAPPα bound ~5 fold more $A\beta_{1-42}$

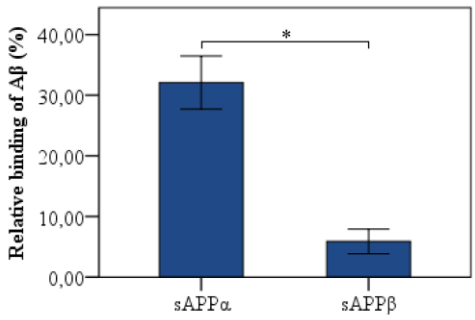

Figure 16: Densitometry results of the Western blots of the pull-down experiments with sAPPα and sAPPβ as bait and $A\beta_{1-42}$ as prey. The bar chart illustrates the mean relative binding percentage of $A\beta_{1-42}$ ± SEM. The results are representative of six independent experiments. Independent sample t-test revealed significant difference between the binding of $A\beta_{1-42}$ by sAPPα compared to sAPPβ (* $P < 0.05$).

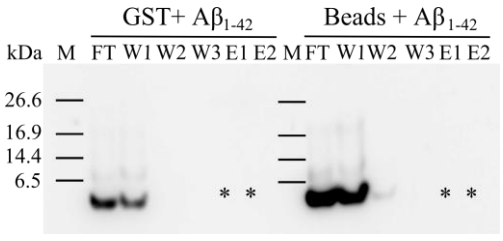

Figure 17: Western blotting with the anti-Aβ antibody 4G8 of the pull down assay with GST and beads as prey and $A\beta_{1-42}$ as bait. The left side illustrates the assay with GST as bait, and the right side the beads as bait. No bands are detected in the eluted fractions E1 and E2 as indicated by the asterisk, revealing no unspecific binding of $A\beta_{1-42}$ to GST or the beads. FT: Flow through, W: Wash, E: Eluted protein fraction.

compared to sAPPβ, it highlighted the possible importance of the unique 16 extra amino acids at the C-terminus of sAPPα in the interaction. These residues are the only differences between the two proteins, and therefore could be the site of the interaction. They also form the first 16 amino acids of Aβ.

In an attempt to characterise the possible interaction site between sAPPα and Aβ. pGEX-6P-3 vectors with six different sAPPα variants (Figure 6) were constructed as well as $Aβ_{1-16}$ and $Aβ_{17-42}$.

4.4 Production of $Aβ_{1-16}$ and $Aβ_{17-42}$

To characterize the interaction site between $Aβ_{1-42}$ and sAPPα, $Aβ_{1-16}$ and $Aβ_{17-42}$ were made. $Aβ_{1-16}$ contains the same 16 amino acids which is unique at the end of sAPPα, and which seem to be important for the interaction. The plasmid with $Aβ_{1-42}$ was isolated and purified for use as template for the PCR production of $Aβ_{1-16}$ and $Aβ_{17-42}$. As seen on the agarose gel Figure 18 the fragments were successfully produced (lanes 2 and 4). No product was produced in the samples with no template, lane 1 and 3, indicating no primer-dimer formation when using the designed primers. The PCR products of $Aβ_{1-16}$ and $Aβ_{17-42}$ both contained an *Xba* I and *Pst* I recognition site therefore the next step was cutting the fragments and pMAL-c2 vectors with these

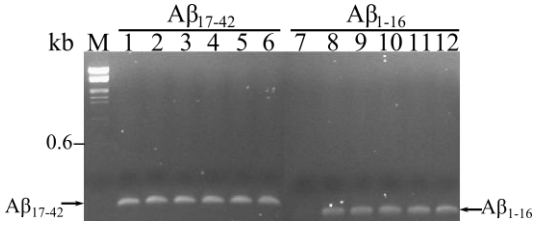

Figure 19: Agarose gel with the PCR screening results. The colonies 1-6 are positive for the insert of $Aβ_{17-42}$, and the colonies 8-12 are positive for the insert $Aβ_{1-16}$. M: λ DNA-*EcoR* I + *Hind* III marker

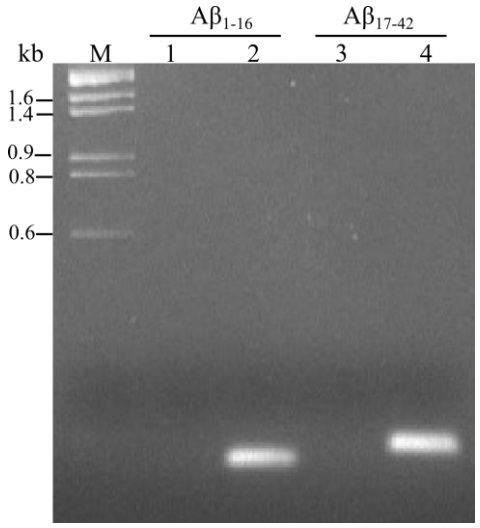

Figure 18: Agarose gel with the PCR results from the production of $Aβ_{1-16}$ and $Aβ_{17-42}$. Lane 1, 3 had no templates DNA, lane 2, 4 had template DNA. M: λ DNA-*EcoR* I + *Hind* III marker

digestion enzymes. After digestion the inserts $Aβ_{1-16}$ and $Aβ_{17-42}$ were ligated with precut pMAL-c2 vectors, and transformed into DH5α bacteria. Many colonies were observed on the plates with transformed bacteria and no colonies were observed on the control plate. Six colonies were therefore screened by PCR with the same primers used for the production of $Aβ_{1-16}$ and $Aβ_{17-42}$ PCR products (Table 1). Figure 19 illustrates the agarose gel of the PCR screening results, five of the six colonies screened for $Aβ_{1-16}$ were found to be positive (lanes 8-12) and all of the 6 $Aβ_{17-42}$ colonies were positive (lanes 1-6). Purified plasmids from three positive colonies of each were subsequently cut with *Xba* I and *Pst* I to confirm that they contained inserts. The small inserts themselves ran off the 1 % (w/v) agarose gel but there was a shift in size of the vectors after they had been cut, see lane 2, 4, 6, 8, 10, and 12 on Figure 20. This implies that all vectors had been positive for either $Aβ_{1-16}$ or $Aβ_{17-42}$. Two clones from each $Aβ_{1-16}$ and $Aβ_{17-42}$ were sent away for sequencing.

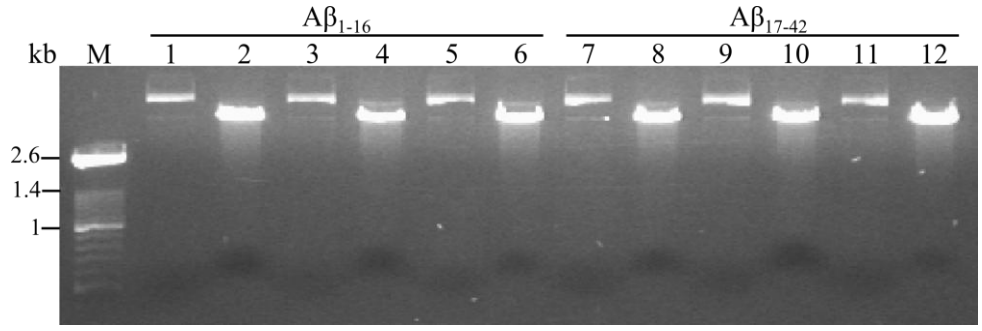

Figure 20: Agarose gel of the digest of three vectors containing $A\beta_{1-16}$, and $A\beta_{17-42}$.which have been purified from positive PCR colonies. Lanes 1, 3, 5, 7, 9, and 11 contain uncut vectors, and lanes 2, 4, 6, 8, 10, and 12 the cut vectors. There is a shift in size after the vectors have been cut, implying that all of the colonies have the insert of either $A\beta_{1-16}$ or $A\beta_{17-42}$.

As seen in Appendix II, containing the sequencing results, both $A\beta_{1-16}$ and $A\beta_{17-42}$ had been successfully cloned into the pMAL-c2 vector, and both contained the factor Xa cleavage site as shown by the blue box and a stop codon shown by the orange box.

DH5α bacteria were then transformed with plasmids containing MBP-$A\beta_{1-16}$ and MBP-$A\beta_{17-42}$. Many colonies were observed on the plates with transformed bacteria and none on the control plate. A colony of each was seeded in LB medium and in response to IPTG both MBP-$A\beta_{1-16}$ and MBP-$A\beta_{17-42}$ were produced. Figure 21 illustrates a Coomassie stained SDS-PAGE gel with both the uninduced (lanes 1 and 3) and induced (lanes 2 and 4) samples. A large amount of a protein is seen in lane 2 and 4 (~45 kDa) representing MBP-$A\beta_{1-16}$ and MBP-$A\beta_{17-42}$, respectively. The procedure for the purification was the same as for $A\beta_{1-42}$, and until the separation from the carrier MBP following factor Xa cleavage the purification-profile looked the same as for $A\beta_{1-42}$ (Figure 9, Figure 10, and Figure 11). To separate $A\beta_{1-16}$ and $A\beta_{17-42}$ from the carrier MBP, RPC was used. Before applying the samples on the RPC column, aggregation of $A\beta_{1-16}$, but not $A\beta_{17-42}$, was observed. $A\beta_{1-16}$ was therefore resolubilised before being applied to the column.

Figure 22 illustrates the fractionation of MBP and $A\beta_{17-42}$ on RPC. A peak is observed in fraction D8, as indicated by the angled arrow on Figure 22A, which is the region where the elution of $A\beta_{17-42}$ was expected. However, when analysing the fractions on SDS-PAGE and with Western blotting (Figure 22B, and C, respectively), it is revealed that it is another protein causing the peak, indicated by an angled arrow on Figure 22B. No $A\beta_{17-42}$ was observed in the flow through (FT), and fraction D4-D7 and D9-D10 was pooled and used in the pull-down assay. The fractionation profile of MBP and $A\beta_{1-16}$ on RPC looked the same as the profile for $A\beta_{17-42}$, see Appendix III, and fraction D4-D6 and D9 was pooled. The concentrations of the pooled $A\beta_{1-16}$ and $A\beta_{17-42}$ were determined, and used in the pull-down assay as prey.

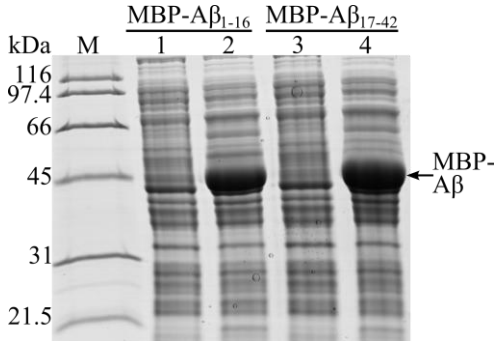

Figure 21: SDS-PAGE gel illustrating uninduced and induced samples of the MBP tagged $A\beta_{1-16}$ and $A\beta_{17-42}$ in DH5α bacteria. M: Broad range marker, 1, 3: Uninduced samples, 2, 4: Induced samples.

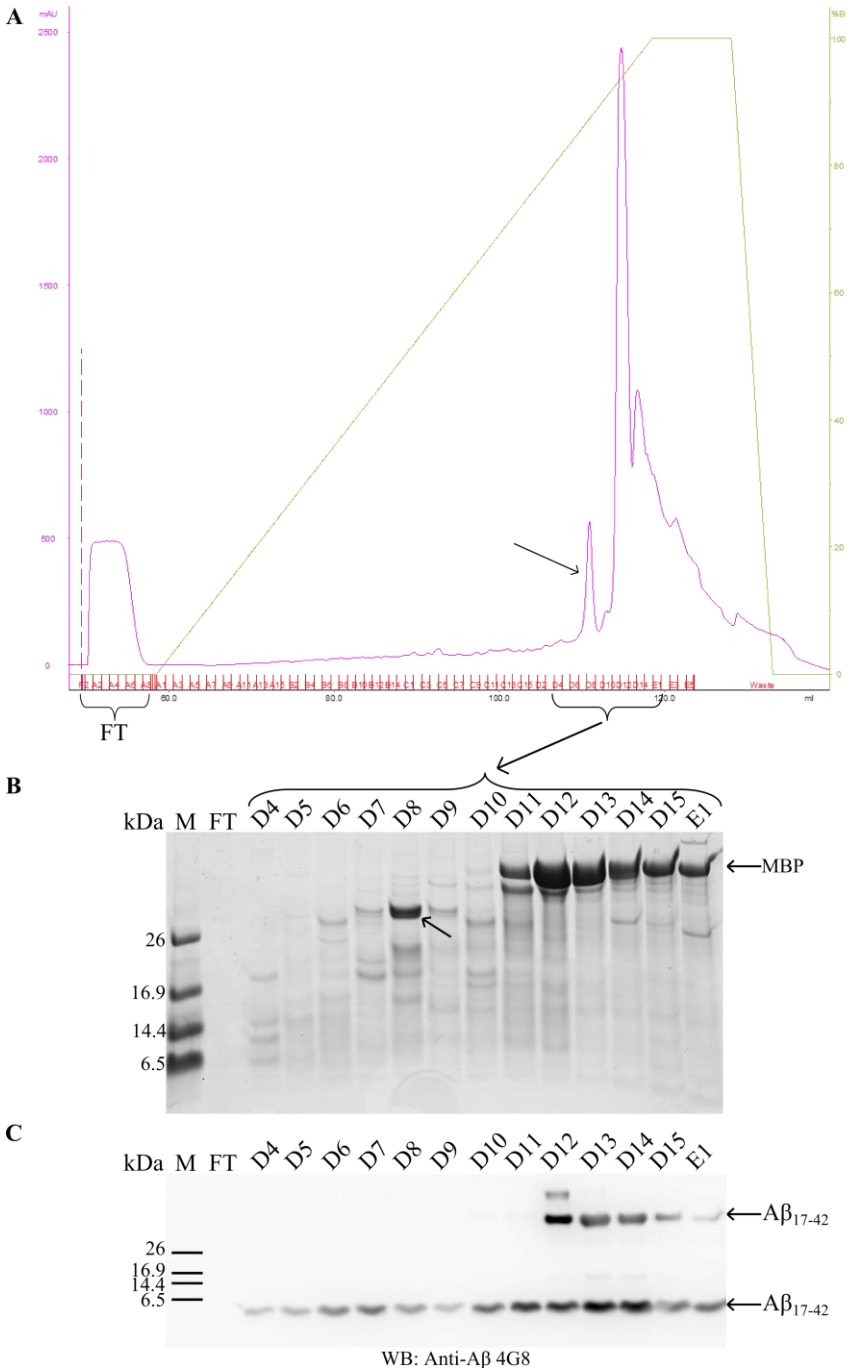

Figure 22: **A**. Fractionation of MBP and $A\beta_{17-42}$ on RPC. The pink trace illustrates the proteins absorbed at 215 nm, and the green trace is the percentage of buffer B that represents the change from 5-50 % acetonitrile. **B.** SDS-PAGE gel analysis of the fractions containing protein, and the flowthrough (FT), both marked by a bracket on A. **C.** Western blotting with the anti-Aβ antibody 4G8 to confirm the identity of the protein. Fraction D4-D7 and D9-D10 was pooled and used in the pull down assay. Fraction D12-D15 and E1 contain uncleaved fusion protein. M: Peptide marker, FT: Flow through.

4.5 GST pull-down assay with $A\beta_{1-16}$ and $A\beta_{17-42}$

The interaction assay was repeated with GST-sAPPα and GST-sAPPβ as bait and $A\beta_{1-16}$ and $A\beta_{17-42}$ as prey. Figure 23 illustrates the Western blotting results from the pull-down assay with $A\beta_{1-16}$ as bait. More $A\beta_{1-16}$ is observed in the eluted fraction (E1) from the pull-down assay with sAPPα

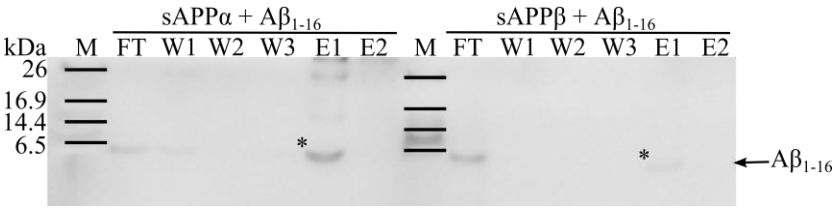

Figure 23: Western blotting with the anti-Aβ antibody 6E10 of the pull down assay using sAPPα and sAPPβ as bait and $Aβ_{1-16}$ as prey. The asterisks indicate bound $Aβ_{1-16}$. M: Peptide marker, FT: Flow through, W: Wash, E: Eluted protein fractions.

as prey compared to the one with sAPPβ as prey. The pull-down was repeated three times, with consistent data despite the quality of the Western blots, Appendix IV. When comparing the intensity of the bands with the interaction assays with full length $Aβ_{1-42}$, they are much fainter despite the proteins were added in the same molar concentration. This indicates that some of the $Aβ_{1-16}$ has been lost during processing.

Collectively, the experiments indicated that more $Aβ_{1-16}$ is bound by sAPPα compared to sAPPβ. When the interaction assay was repeated with $Aβ_{17-42}$, no proteins were detected in any of the fractions. Figure 24A illustrates the 3rd attempt to detect $Aβ_{17-42}$ with the 4G8 antibody. No $Aβ_{17-42}$ was detected in any of the fractions, flow through, washes, or elutes. A fraction of the beads (B) was also analysed on the Western blot, and still no $Aβ_{17-42}$ was detected.

To investigate where the loss of protein had occurred, the detection of $Aβ_{17-42}$ was tested with a Western blot at the same time as when the $Aβ_{17-42}$ was applied to the pull-down assay. As seen in Figure 24B lanes 1 and 2, the protein could be detected at this point, indicating that intact $Aβ_{17-42}$ had been present in the interaction experiments.

4.6 Production of sAPPα variants

pcDNA3.1D/V5-His-TOPO vectors containing the different sAPPα variants were provided from the research group. They were digested with the restriction enzymes *Sma* I and *Not* I releasing a 1.8 Kb fragment containing the sAPPα variant sequence, as indicated by the arrow on Figure 25A. The 1.8 kDa fragment was purified and the concentration measured.

Then the purified fragment containing the sAPPα variant sequence was cloned into a pGEX-6P-3 vector, which had been cut with the same restriction enzymes. This enabled the production of GST tagged sAPPα variants, in response to the addition of IPTG.

To increase the frequency of recombinant vectors containing the fragments of the sAPPα variant, the vectors were incubated

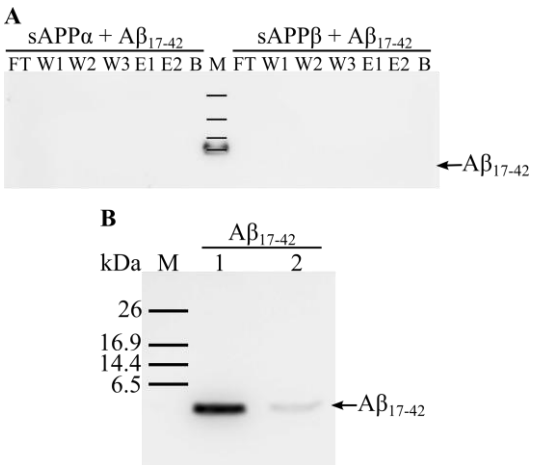

Figure 24: **A**. Western blotting with the anti-Aβ antibody 4G8 of the pull down assay with sAPPα and sAPPβ as bait and $Aβ_{17-42}$ as prey. No bands are detected. M: Peptide marker, FT: Flow through, W: Wash, E: Eluted protein fractions, B: Beads after elute of proteins. **B.** Test of input protein for the interaction assay. M: Peptide marker, 1: 0.84 µg $Aβ_{17-42}$, 2: 0.084 µg $Aβ_{17-42}$.

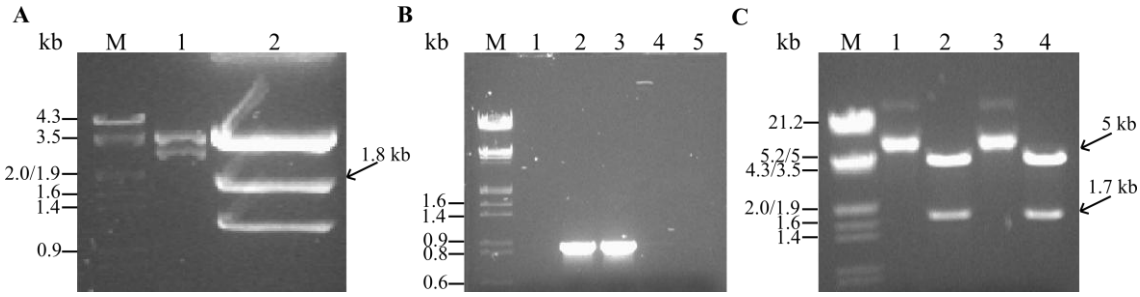

Figure 25: **A**. Agarose gel of the digest of the pcDNA3.1D/V5-His-TOPO vector containing a sAPP variant. The arrow indicate the 1.8 Kb band which was purified. 1: 1st digest (*Sma* I), 2: 2nd digest (*Not* I). **B**. Agarose gel with the PCR screening results. The screened colony in lanes 2 and 3 was found positive for the insert of a sAPP variant. 1-5: PCR screened colonies. **C.** Agarose gel of the digest of the plasmids purified from colonies, lanes 2 and 3 figure B. The arrows mark the 5 kb and 1.7 kb bands which indicate the plasmid contains the insert. 1: Plasmid from colony 2 figure B, 2: Cut plasmid from colony 2 figure B, 3: Plasmid from colony 3 figure B, 4: Cut plasmid from colony 3 figure B. M: λ DNA/*EcoR* I + *Hind* III marker.

with *Sal* I, which cleaves all vector molecules without the insert.

The products from the ligation were then transformed into DH5α bacteria and colonies of the transformed bacteria were screened for vectors containing the cloned insert, using a pGEX forward and APP933-1018 reverse primer. As seen on the agarose gel, Figure 25B, two colonies were found positive for the insert of the variant.

The plasmids from the positive clones were isolated. To further confirm the vectors contained the correct insert, they were digested with the restriction enzymes *EcoR* I and *Bgl* II. If the vectors were positive for the insert, two bands of 5 kb and 1.7 kb, respectively should be revealed. Uncut and cut samples were analysed on an agarose gel, and both colonies were found to be positive, see Figure 25C. The positive

Figure 26: **A**. An illustration of how three primers, pGEX forwad, $APP_{500-521}$, and pGEX reverse are used to sequence the sequence of the sAPPα variants. **B**. A representative segment of the sequencing data, showing the quality. **C**. All the sAPPα variants contain a silent mutation, marked by the blue box, GAA have been changed to GAG. Both code for glutamic acid.

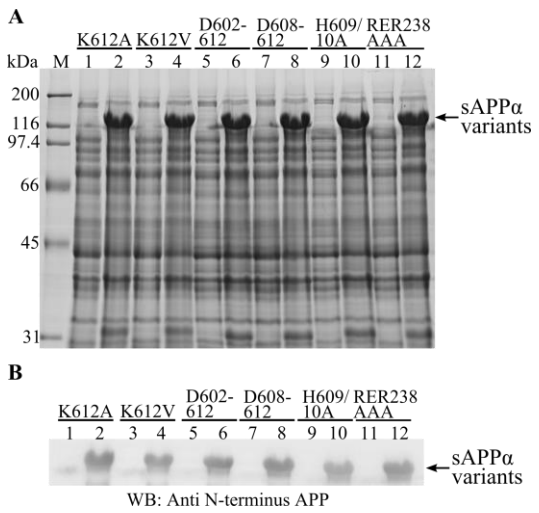

Figure 27: **A.** SDS-PAGE gel illustrating uninduced and induced samples of the GST tagged sAPP variants in BL21 bacteria. **B.** Western blotting (WB), anti-N-terminus APP to confirm the identity of the protein. M: Broad range marker, 1,3,5,7,9,11: Uninduced samples, 2,4,6,8,10, 12: Induced samples.

plasmids were sequenced to confirm the presence of the sAPPα variant sequence and the absence of any errors introduced. Three primers were used to cover the sAPPα variant sequence as illustrated on Figure 26A. The sequencing data were analysed for point mutations. Figure 26B illustrate a representative segment of the sequencing data, showing good quality. At least one colony from each sAPPα variant was found to contain the correct insert. However, all of the pGEX-6P-3 vectors with a sAPPα variant contained the same silent mutation. This is illustrated on Figure 26C, where the sequence GAA when sequenced was GAG in the sAPPα variants. The mutation was analysed, revealing that both code for glutamic acid, and all of the variants were therefore considered to have the correct sequence.

All of the GST tagged sAPPα variants were successfully expressed in transformed BL21 cells in response to IPTG, see Figure 27A, lanes 1, 3, 5, 7, 9, and 11 (~116 kDa). The identity of the proteins were confirmed with, a Western blot using the antibody to the N-terminus of APP, Figure 27B.

In order to purify the GST tagged sAPPα variants they were mixed with glutathione Sepharose 4B beads. The purification profiles for the sAPPα variants (not shown) were the same as for sAPPα, Figure 8.

4.7 GST pull-down assays with the sAPPα variants

The GST pull-down assay was then repeated with the GST-tagged sAPPα variants as bait and $A\beta_{1-42}$ as prey. The interaction assay with each variant was repeated four times (Figure 28, Figure 29, Figure 30, and Figure 31).

The binding of $A\beta_{1-42}$ was reduced with the sAPPα variants D608-612 and D602-612, see Figure 29A and B, and Appendix V, A and B. To give a more detailed picture of the binding, the results were analysed by densitometry. As seen in Figure 28 the binding of $A\beta_{1-42}$ was significantly reduced with ~2.5 fold when the last 5 amino acids

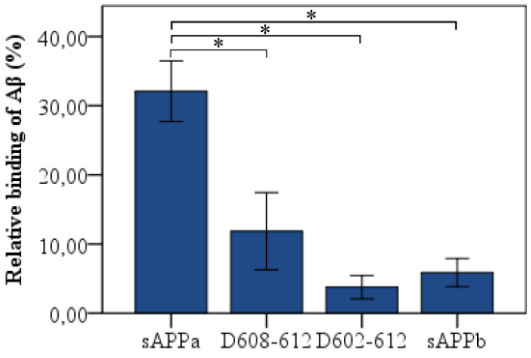

Figure 28: Densitometry results of the Western blots of the pull-down experiments with sAPPα, sAPPβ and the deletion variants D608-612 and 602-612 as bait and $A\beta_{1-42}$ as prey. The bar chart illustrates the mean relative binding percentage of $A\beta_{1-42}$ ± SEM. The results are representative of six independent experiments for sAPPα, and sAPPβ, and four for the variants. Independent sample t-test revealed significant difference between the binding of $A\beta_{1-42}$ by sAPPα compared to sAPPβ and the two variants (* $P < 0.05$).

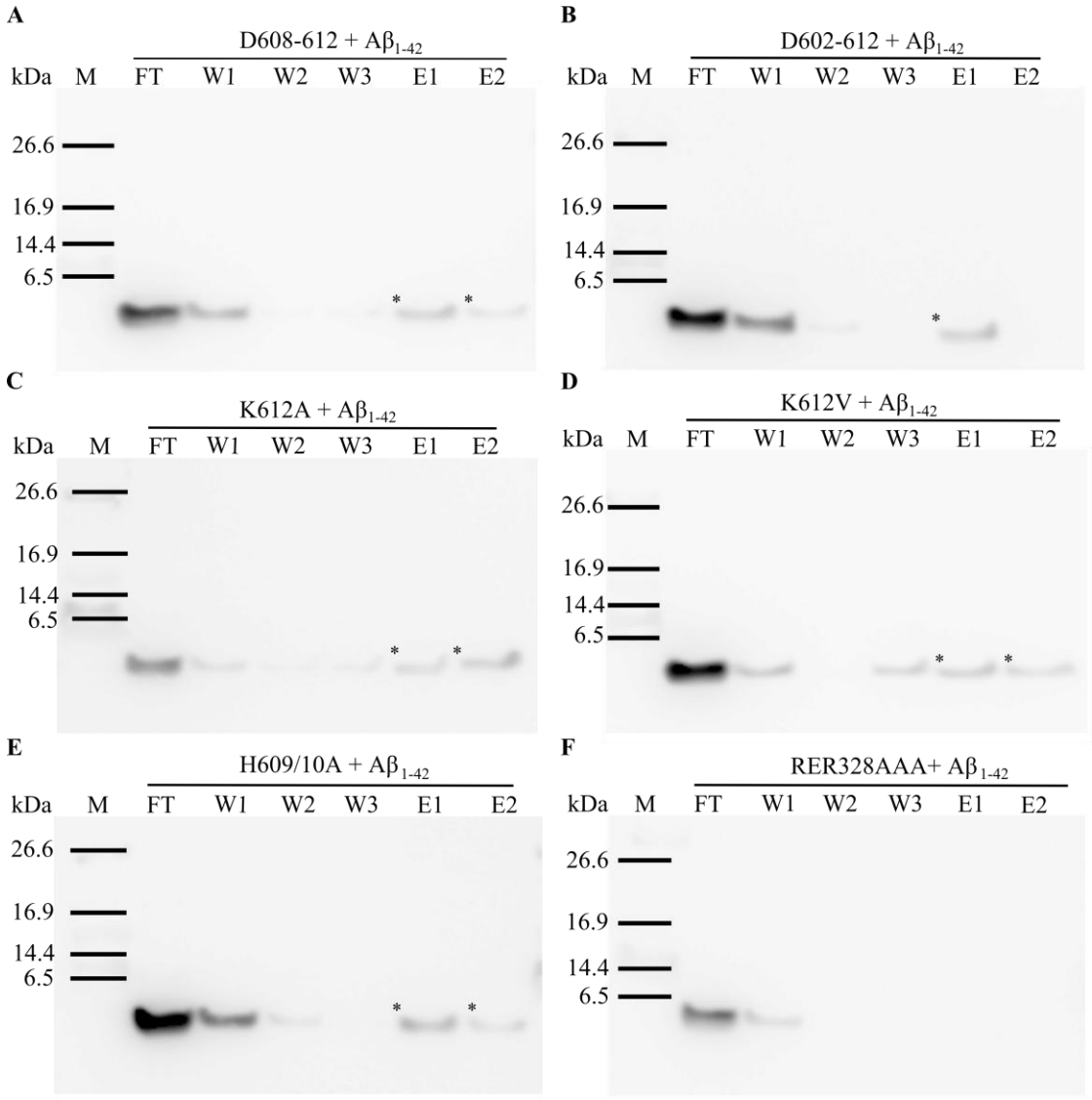

Figure 29: Western blotting with the anti-Aβ antibody 4G8 of one representative pull down assay for each of the interaction assays using the sAPPα variants: A. D608-612, B. D602-612, C. K612A, D. K612V, E. H609/10A, and F. RER328-330AAA as bait and $A\beta_{1-42}$ as prey. The asterisks indicate bound $A\beta_{1-42}$. M. Peptide marker, FT: Flow through, W: Wash, E: Eluted protein fractions.

of sAPPα were deleted (D608-612) compared to the full-length sAPPα. When a further 5 amino acids were deleted (D602-612) the binding of $A\beta_{1-42}$ was reduced to a level similar to that of sAPPβ, Figure 28. This further emphasised the importance of the unique 16 amino acids at the C-terminus of sAPPα.

Figure 29C and D and Appendix V, C and D illustrate the immunoblots of the interaction of $A\beta_{1-42}$ with the sAPPα variants K612A, and K612V, and the asterisk indicates the eluted fractions containing $A\beta_{1-42}$. The densitometry analysis, Figure 30, revealed a reduction in the binding of $A\beta_{1-42}$ of ~1.7 and ~3 fold for K612A and K612V, respectively compared to sAPPα. The reduction in binding is statistically significant for the K612V variant but not for the K612A variant.

By changing each of the two histidines, at position 609/10 (a putative metal ion binding site) to alanine (H609/10A), the binding of $A\beta_{1-42}$ is significantly reduced compared to sAPPα. The proportion of binding was at a similar level of that observed for

the D608-612, where the two histidines also have been deleted, see Figure 31.

The last tested variant was sAPPα with the RER328-330AAA mutation. RER has been the subject of much interest for the functional activity of sAPPα [Mileusnic *et al.*, 2005; Ninomiya *et al.*, 1993]. Figure 29F illustrates the interaction assay with RER328-330AAA GST-sAPPα variant as bait and $A\beta_{1-42}$ as prey, no interaction was observed in the first interaction assay, however in the repeats see Appendix V, F a small proportion of binding was observed. After analysis of the results with-densitometry, it was found that RER328-330AAA binds approximately the same amount of $A\beta_{1-42}$ as sAPPβ as seen on the bar chart Figure 30.

In summary, the last 16 amino acids of sAPPα seem to be important for the binding of $A\beta_{1-42}$ since the deletions and amino acid substitutions reduced the binding potential of sAPPα to $A\beta_{1-42}$ (Figure 29). However, the more N terminal RER motif at position 328-330 in the molecule plays some role as yet unexplained mechanism shown by its effect on the interaction despite its distant location.

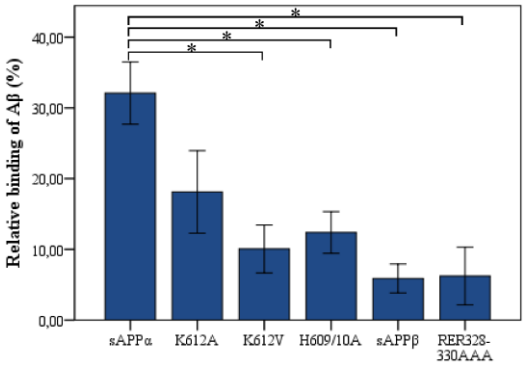

Figure 30: Densitometry results of the Western blots of each of the pull-down experiments with sAPPα, sAPPβ and the substitution variants K612A, K612V, H609/10A RER328-330AAA as bait and $A\beta_{1-42}$ as prey. The bar chart illustrates the mean relative binding percentage of $A\beta_{1-42}$ ± SEM. The results are representative of six independent experiments for sAPPα and sAPPβ, and four for the variants. Independent sample t-test revealed significant difference between the binding of $A\beta_{1-42}$ by sAPPα compared to sAPPβ and all of the variants except K612A (* $P < 0.05$).

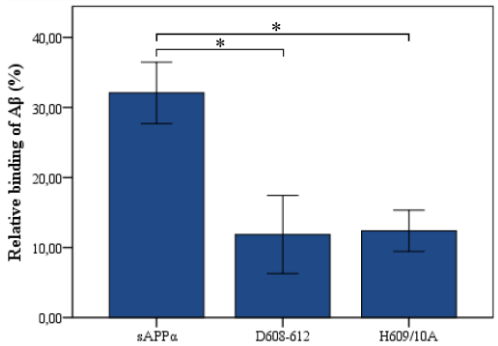

Figure 31: Densitometry results of the Western blots of each of the pull-down experiments with sAPPα, and the variants D608-612, and H609/10A as bait and $A\beta_{1-42}$ as prey. Each bar is represented as the mean ± SEM and is representative of six independent experiments for sAPPα, and four for D608-612 and 602-612. Independent sample t-test revealed significant difference between the binding of $A\beta_{1-42}$ by sAPPα and the two variants (* $P < 0.05$).

5 Discussion

5.1 Production of GST-tagged sAPPα variants

The GST-tagged sAPP variant proteins (Figure 6, Material and Methods) were successfully produced in bacteria (strain BL21). When purifying the proteins using the glutathione Sepharose 4B beads, a fraction of the proteins did not bind to the beads and was found in the flow through and washes. This could have been caused by inappropriately folded proteins, masking, or a steric hindrance of the GST-tag, interfering with the glutathione on the beads.

While there were minor contaminating bands in each of the eluted fractions (Figure 8, Results), the degree of purity was acceptable for the purpose of this study. The contaminating bands could be caused by unspecific binding of bacterial proteins to the beads or co-purification of chaperones, that are involved in protein folding, with the GST-tagged sAPP variants [Machrey-Nagel, 2010].

5.2 Interaction of GST-sAPPα with sAPPα

In the pull-down assay with GST-tagged sAPPα as bait and untagged sAPPα as prey no interaction between the two proteins was observed. This was somewhat surprising as it contradicts with the proposed mechanism by Gralle *et al*., 2009 who suggeted that the disruption of the APP dimer is through direct interaction by sAPPα (Figure 3, Introduction), corresponding to binding of sAPPα to its homologous sequence within the precursor APP [Gralle *et al.*, 2009]. sAPPα has also been found to form dimers in solution and the addition of heparin increases the proportion of sAPPα dimers [Gralle *et al.*, 2006]. Moreover, the formation of APP dimers is proposed to involve the E1 and E2 domains [Xue *et al.*, 2011; Soba *et al.*, 2005]. These two regions are also part of sAPPα and one could therefore speculate that sAPPα also would form dimers through these regions. However no interaction was observed under the conditions used in this study. This could be due to the fact that GST-tagged sAPPα is produced in bacteria, and lacks the post-translational modifications present on the prey sAPPα, produced in cultured human cells. The GST-tag might also interfere with the possible binding. No binding was observed when untagged sAPPβ was used as prey, neither when GST-tagged sAPPβ was used as bait and untagged sAPPα as prey. These results do not rule out the possibility of interaction of sAPPα or sAPPβ with itself, since it might be due to the design of this experimental pull-down strategy.

5.3 Interaction of the GST-sAPP variants with $A\beta_{1-42}$

The pull-down assays with GST-sAPPα or GST-sAPPβ as bait and $A\beta_{1-42}$ as prey by contrast revealed highly significant binding of $A\beta_{1-42}$ by sAPPα but not with sAPPβ. This further emphasized the potential importance of the unique 16 amino acids at the C-terminal of sAPPα, since these residues are the only difference between the two proteins. Nevertheless, a small proportion of $A\beta_{1-42}$ was bound by GST-sAPPβ. The binding could be ascribed to binding of $A\beta_{1-42}$ to sequences within the N-terminal domain since Von Nostrand *et al*., 2002 have found that the N-terminal region (18-119) of APP mediates binding of APP to the fibrillar forms of Aβ. Furthermore, His^{110}, Val^{112}, and Ile^{113} comprise a motif that mediates the binding of the fibrillar form of Aβ to APP. [Van Nostrand *et al.*,

2002] This region is found in both sAPPα and sAPPβ, and could therefore also contribute to a secondary binding of $A\beta_{1-42}$.

The primary interaction could be a previously unrecognised novel function of sAPPα, in accordance with the fact that sAPPα has previously been shown to protect cell cultures against Aβ induce toxicity [Furukawa *et al.*, 1996; Guo *et al.*, 1998]. Some of this protection could possibly be assigned to the binding of Aβ by sAPPα. It should be noted, however, Shaked *et al*., 2006 have previously shown that Aβ binds to its homologous sequence (596-624) on the precursor protein APP. In the present study indication of binding of $A\beta_{1-42}$ to residues 597-612 of sAPPα was revealed.

To further characterize the possible interaction site between sAPPα and $A\beta_{1-42}$, and its characteristics, five different GST-tagged sAPPα variants with changes in the critical 16 amino acid region were constructed, as well as one within a motif (RER328-330AAA) of much functional interest (Figure 6, Materials and Methods).

It has previously been shown that the heparin binding domain -VHHQK- (residue 608-612) is particularly effective at mediating the neuroprotective effect of sAPPα against excitotoxicity and Aβ toxicity [Furukawa *et al.*, 1996]. This correlates with the observations that the binding of Aβ is reduced when the two histidines (H609/10A) are substituted with two alanines. The same reduction in binding was observed when the last five amino acids were deleted (D608-612), corresponding to deletion of the heparin binding domain containing the two histidines. This indicates that this region and especially the two histidines are important for the interaction between $A\beta_{1-42}$ and sAPPα. When deleting a further five amino acids (D602-612) the binding of $A\beta_{1-42}$ was reduced to the same level as sAPPβ. This implies that amino acids 602-612 contain the residues important for the interaction, and not amino acids 597-602 (the only difference between sAPPβ and D602-612).

It has previously been shown in the Tate lab, that by changing the last amino acid, lysine, of sAPPα to either alanine or valine the neuroprotective effect of sAPPα is lost [Singh, M. (2010) B. BioMedSci, Honours thesis]. In the present study, a reduction in the binding of $A\beta_{1-42}$ was observed with the two sAPPα variants K612A and K612V compared to sAPPα. Lysine is often involved in the binding or active site of a protein [Russell, 2003], which correlates with the finding that the last 5 amino acids are important for the binding. Moreover, lysine is a polar amino acid and both the substitutions alanine and valine are of different character, neutral and non polar respectively. These are typically part of a protein that is not involved in protein-protein interaction activity, thus a reduction in sAPPα binding could be ascribed to the change in character of the C-terminal amino acid. [Russell, 2003] The neutral amino acid, alanine, can be used to substitute other amino acids in proteins without major disruption of structure, and here, the reduction was not significantly different from the binding of $A\beta_{1-42}$ by sAPPα when lysine was substituted. By contrast, valine, being non polar could cause a larger effect in the protein structure or within an important motif of the protein interaction. This correlates with the finding that K612V significantly reduced the binding of $A\beta_{1-42}$ compared to sAPPα.

The interaction assay was also repeated with the sAPPα variant with the RER328-330AAA mutation as bait and $A\beta_{1-42}$ as prey. The RER motif have been found to be the smallest sequence of sAPPα respon-

sible for the neurotrophic property [Ninomiya *et al.*, 1993] and some of the neuroprotective effects [Mileusnic *et al.*, 2005]. The binding of $A\beta_{1-42}$ was reduced to a similar level as that of sAPPβ. This was somehow surprising due to the distant location of the RER from the 16 amino acids at the C-terminus of sAPPα, the proposed site of the interaction. It has been found that when dealing with large proteins, that contain several different domains like sAPPα, the activity of one domain might depend on the presence of another domain, even if the two domains are far apart in the primary sequence [Fedorov and Baldwin, 1999]. This could be the case with the RER motif and the 16 amino acids at the C-terminal of sAPPα indicating that the RER motif is necessary for the binding of $A\beta_{1-42}$ to the C-terminal. This has not been confirmed, and further investigations are needed.

5.4 Production of $A\beta_{1-16}$ and $A\beta_{17-42}$

In order to further characterize the interaction site between sAPPα and $A\beta_{1-42}$, $A\beta_{1-16}$ and $A\beta_{17-42}$ were constructed. $A\beta_{1-16}$ contains the same residues as the 16 unique amino acids at the C-terminus of sAPPα, and $A\beta_{17-42}$ corresponds to the P3 fragment, generated through the amyloidogenic pathway (Figure 2, Introduction). During the production of these two Aβ fragments, self aggregation of $A\beta_{1.-16}$ was observed. $A\beta_{1-42}$ is prone to aggregation, it has been found that residues 18-42 are responsible through formation of a β-strand-turn-β-strand motif. With the two amino acid regions 18-26 and 31-42 being responsible for the connection of the β-strands. These can further aggregate into fibrils. [Luhrs *et al.*, 2005] The fact that aggregation of $A\beta_{1-16}$ was observed does not correlate with these observations since the residues 18-26 and 31-42 are not part of $A\beta_{1-16}$. However, as indicated by the present experiments, $A\beta_{1-16}$ could interact with its homologous sequence on sAPPα. Shaked *et al.*, 2006 also found that that Aβ can interact with its homologous region on APP (597-624), this region is also part of $A\beta_{1-16}$ [Shaked *et al.*, 2006]. An interaction between two $A\beta_{1-16}$ proteins could therefore be the explanation of the aggregation observed during the production of $A\beta_{1-16}$.

5.5 Interaction of sAPPα with $A\beta_{1-16}$ and $A\beta_{17-42}$

When performing the pull-down assays using GST-sAPPα or GST-sAPPβ as bait and $A\beta_{1-16}$ as prey, indication of more binding of $A\beta_{1-16}$ by sAPPα was observed when compared to the binding by sAPPβ. However, the Western blots revealed relatively faint bands (Figure 23), compared with the interaction assays with full-length $A\beta_{1-42}$, indicating less protein. However, both $A\beta_{1-16}$ and $A\beta_{17-42}$ were added in sufficient amounts (2.25 nmoles), this implies that some of the $A\beta_{1-16}$ has been lost during the experiment. This is likely due to aggregation as explained in section 5.4

I was not able to detect $A\beta_{17-42}$ in any of the fractions from the pull-down assays with GST-sAPPα or GST-sAPPβ as bait and $A\beta_{17-42}$ as prey. The amount of $A\beta_{17-42}$ added was also the same as for the full-length Aβ, (2.25 nmoles), and therefore the 4G8 antibody that recognize amino acid 17-24 should be able to detect the $A\beta_{17-42}$ like the full length $A\beta_{1-42}$. At the time of the addition of the protein to the pull-down assay, an aliquot of the protein was removed and run on a SDS-PAGE gel for Western blot analysis. The protein was easily detected at this point, indicating that intact $A\beta_{17-42}$ had been present in the inter-

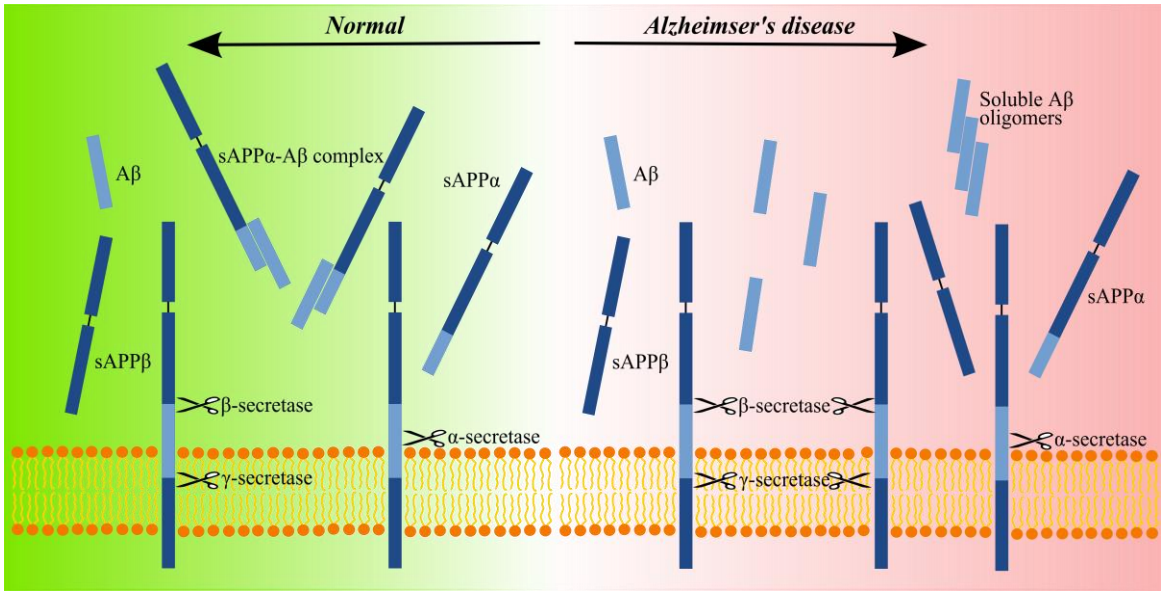

Figure 32: Hypothetical model of the action of APPα. *Left*, in the normal brain equilibrium between sAPPα and Aβ is maintained by binding of Aβ trough the C-terminus of sAPPα. *Right*, in the Alzheimer's disease brain an increased β- and γ-secretase activity and decreased α-secretase activity is observed, resulting in the production of more Aβ and less sAPPα. Thereby, sAPPα can no longer maintain the equilibrium by binding of Aβ.

action experiments. Additionally, a fraction of the glutathione sepharose 4B beads after elution of the proteins was tested, and no protein was detected still bound to these, ruling out unspecific tight binding of $A\beta_{17-42}$ to the beads. An explanation for the lack of detection could be the formation of aggregated $A\beta_{17-42}$ during the incubation with GST-sAPPα or GST-sAPPβ. The residues responsible for the aggregation are likely to be, as mentioned above 18-26 and 31-42 [Luhrs *et al.*, 2005], both of which are part of $A\beta_{17-42}$.

5.6 Perspective

The present study suggests a novel explanation for the neuroprotective effect of the protein sAPPα. sAPPα has previously been shown to interact with APP [Gralle *et al.*, 2009], very recently β-secretase [Obregon *et al.*, 2012], and integrin β1 [Young-Pearse *et al.*, 2008]. These interactions relate to potential mechanisms of neuroprotection, regulation of Aβ production, and modulation of neurite outgrowth respectively. An addition to an already complex function of sAPPα could be the binding of $A\beta_{1-42}$ when concentrations are exceeding normal physiological limits. This binding of Aβ could be part of a regulatory circuit involving sAPPα to keep sAPPα and Aβ in a balanced equilibrium. In AD, the concentration of sAPPα has been shown to decrease, and the concentration of Aβ to increase. This distortion to the equilibrium results in sAPPα no longer can maintain the equilibrium with Aβ. The proposed mechanism is illustrated in Figure 32. To confirm or disconfirm the proposed mechanism, further investigations of the function of the interaction between $A\beta_{1-42}$ and sAPPα are needed.

6 Conclusion

In the present study, a novel explanation for the neuroprotective effect of sAPPα is suggested. The pull-down assay revealed binding of sAPPα to $A\beta_{1-42}$. Furthermore, sAPPα binds significantly more $A\beta_{1-42}$ than sAPPβ implying that the main interaction involves the 16 amino acids positioned at the C-terminus of sAPPα. This was further supported by the interaction assays with the sAPPα variants revealing the importance of the metal ion binding site VHHQK at position 608-612. Deletion of ten amino acids at the C-terminus of sAPPα reduced the binding of $A\beta_{1-42}$ to a similar level as that found for sAPPβ, indicating that the interaction with $A\beta_{1-42}$ involve binding to residues 602-612. The binding was shown to rely on an intact RER motif (residues 328-330), since the sAPPα variant with the RER328-330AAA substitution caused a significant decrease in the binding of $A\beta_{1-42}$.

The interaction of sAPPα with $A\beta_{1-42}$, may contribute to the neuroprotective effect of sAPPα by keeping sAPPα and $A\beta_{1-42}$ in a balanced equilibrium. In order to provide further insight into the mechanisms of the interaction and its involvement in the normal brain and in AD, further investigations are needed.

7 Reference

Alzheimerforeningen. *Fakta om antal demente i Danmark* [Online]. Available: http://www.alzheimer.dk/index.php?pk_menu=963&pk_knowledge=59 [Accessed 1.11.2011 2011].

American-Health-Assistance-Foundation. 2000-2012. *Plaques and Tangles* [Online]. Available: http://www.ahaf.org/alzheimers/about/understanding/plaques-and-tangles.html [Accessed 07.03 2012].

Aydin, D., Filippov, M. A., Tschape, J. A., Gretz, N., Prinz, M., Eils, R., Brors, B. & Muller, U. C. 2011. **Comparative transcriptome profiling of amyloid precursor protein family members in the adult cortex**. *BMC Genomics,* 12**,** 160.

Baratchi, S., Evans, J., Tate, W. P., Abraham, W. C. & Connor, B. 2011. **Secreted amyloid precursor proteins promote proliferation and glial differentiation of adult hippocampal neural progenitor cells**. *Hippocampus*.

Beher, D., Hesse, L., Masters, C. L. & Multhaup, G. 1996. **Regulation of amyloid protein precursor (APP) binding to collagen and mapping of the binding sites on APP and collagen type I**. *J Biol Chem,* 271**,** 1613-20.

Chasseigneaux, S., Dinc, L., Rose, C., Chabret, C., Coulpier, F., Topilko, P., Mauger, G. & Allinquant, B. 2011. **Secreted amyloid precursor protein beta and secreted amyloid precursor protein alpha induce axon outgrowth in vitro through Egr1 signaling pathway**. *PLoS One,* 6**,** e16301.

Eggert, S., Midthune, B., Cottrell, B. & Koo, E. H. 2009. **Induced dimerization of the amyloid precursor protein leads to decreased amyloid-beta protein production**. *J Biol Chem,* 284**,** 28943-52.

Fedorov, A. N. & Baldwin, T. O. 1999. **Process of biosynthetic protein folding determines the rapid formation of native structure**. *J Mol Biol,* 294**,** 579-86.

Furukawa, K., Sopher, B. L., Rydel, R. E., Begley, J. G., Pham, D. G., Martin, G. M., Fox, M. & Mattson, M. P. 1996. **Increased activity-regulating and neuroprotective efficacy of alpha-secretase-derived secreted amyloid precursor protein conferred by a C-terminal heparin-binding domain**. *J Neurochem,* 67**,** 1882-96.

Gabelle, A., Roche, S., Geny, C., Bennys, K., Labauge, P., Tholance, Y., Quadrio, I., Tiers, L., Gor, B., Chaulet, C., Vighetto, A., Croisile, B., Krolak-Salmon, P., Touchon, J., Perret-Liaudet, A. & Lehmann, S. 2010. **Correlations between soluble alpha/beta forms of amyloid precursor protein and Abeta38, 40, and 42 in human cerebrospinal fluid**. *Brain Res,* 1357**,** 175-83.

Gakhar-Koppole, N., Hundeshagen, P., Mandl, C., Weyer, S. W., Allinquant, B., Muller, U. & Ciccolini, F. 2008. **Activity requires soluble amyloid precursor protein alpha to promote neurite outgrowth in neural stem cell-derived neurons via activation of the MAPK pathway**. *Eur J Neurosci,* 28**,** 871-82.

Giuffrida, M. L., Caraci, F., Pignataro, B., Cataldo, S., De Bona, P., Bruno, V., Molinaro, G., Pappalardo, G., Messina, A., Palmigiano, A., Garozzo, D., Nicoletti, F., Rizzarelli, E. & Copani, A. 2009. **Beta-amyloid monomers are neuroprotective**. *J Neurosci,* 29**,** 10582-7.

Goodman, Y. & Mattson, M. P. 1994. **Secreted forms of beta-amyloid precursor protein protect hippocampal neurons against amyloid beta-peptide-induced oxidative injury**. *Exp Neurol,* 128**,** 1-12.

Gralle, M., Botelho, M. G. & Wouters, F. S. 2009. **Neuroprotective secreted amyloid precursor protein acts by disrupting amyloid precursor protein dimers**. *J Biol Chem,* 284**,** 15016-25.

Gralle, M., Oliveira, C. L., Guerreiro, L. H., Mckinstry, W. J., Galatis, D., Masters, C. L., Cappai, R., Parker, M. W., Ramos, C. H., Torriani, I. & Ferreira, S. T. 2006. **Solution conformation and heparin-induced dimerization of the full-length extracellular domain of the human amyloid precursor protein**. *J Mol Biol,* 357**,** 493-508.

Gregory, G. C. & Halliday, G. M. 2005. **What is the dominant Abeta species in human brain tissue? A review**. *Neurotox Res,* 7**,** 29-41.

Grubbs, F. E. 1969. **Procedure for Detecting Outlying Observations in Samples** *Technometrics,* 11**,** 1-21.

Guo, Q., Li, H., Gaddam, S. S., Justice, N. J., Robertson, C. S. & Zheng, H. 2012. **Amyloid precursor protein revisited: neuron-specific expression and highly stable nature of soluble derivatives**. *J Biol Chem,* 287**,** 2437-45.

Guo, Q., Robinson, N. & Mattson, M. P. 1998. **Secreted beta-amyloid precursor protein counteracts the proapoptotic action of mutant presenilin-1 by activation of NF-kappaB and stabilization of calcium homeostasis**. *J Biol Chem,* 273**,** 12341-51.

Hardy, J. & Selkoe, D. J. 2002. **The amyloid hypothesis of Alzheimer's disease: progress and problems on the road to therapeutics**. *Science,* 297**,** 353-6.

Holtzman, D. M., Morris, J. C. & Goate, A. M. 2011. **Alzheimer's disease: the challenge of the second century**. *Sci Transl Med,* 3**,** 77sr1.

Haas, C., Cazorla, P., Miguel, C. D., Valdivieso, F. & Vazquez, J. 1997. **Apolipoprotein E forms stable complexes with recombinant Alzheimer's disease beta-amyloid precursor protein**. *Biochem J,* 325 (Pt 1)**,** 169-75.

Ishida, A., Furukawa, K., Keller, J. N. & Mattson, M. P. 1997. **Secreted form of beta-amyloid precursor protein shifts the frequency dependency for induction of LTD, and enhances LTP in hippocampal slices**. *Neuroreport,* 8**,** 2133-7.

Jagust, W. J. & Mormino, E. C. 2011. **Lifespan brain activity, beta-amyloid, and Alzheimer's disease**. *Trends Cogn Sci,* 15**,** 520-6.

Kamenetz, F., Tomita, T., Hsieh, H., Seabrook, G., Borchelt, D., Iwatsubo, T., Sisodia, S. & Malinow, R. 2003. **APP processing and synaptic function**. *Neuron,* 37**,** 925-37.

Libeu, C. P., Poksay, K. S., John, V. & Bredesen, D. E. 2011. **Structural and functional alterations in amyloid-beta precursor protein induced by amyloid-beta peptides**. *J Alzheimers Dis,* 25**,** 547-66.

Lourenco, F. C., Galvan, V., Fombonne, J., Corset, V., Llambi, F., Muller, U., Bredesen, D. E. & Mehlen, P. 2009. **Netrin-1 interacts with amyloid precursor protein and regulates amyloid-beta production**. *Cell Death Differ,* 16**,** 655-63.

Luhrs, T., Ritter, C., Adrian, M., Riek-Loher, D., Bohrmann, B., Dobeli, H., Schubert, D. & Riek, R. 2005. **3D structure of Alzheimer's amyloid-beta(1-42) fibrils**. *Proc Natl Acad Sci U S A,* 102**,** 17342-7.

Machrey-Nagel. 2010. *Purification of GST-tagged proteins* [Online]. Available: http://www.mn-net.com/Portals/8/attachments/Redakteure_Bio/Protocols/Protino/UM_ProtinoGST4BColumns.pdf [Accessed 24.05 2012].

Marsden, I. T., Minamide, L. S. & Bamburg, J. R. 2011. **Amyloid-beta-induced amyloid-beta secretion: a possible feed-forward mechanism in Alzheimer's Disease**. *J Alzheimers Dis,* 24**,** 681-91.

Masters, C. L., Simms, G., Weinman, N. A., Multhaup, G., Mcdonald, B. L. & Beyreuther, K. 1985. **Amyloid plaque core protein in Alzheimer disease and Down syndrome**. *Proc Natl Acad Sci U S A,* 82**,** 4245-9.

Mileusnic, R., Lancashire, C. L. & Rose, S. P. 2005. **Amyloid precursor protein: from synaptic plasticity to Alzheimer's disease**. *Ann N Y Acad Sci,* 1048**,** 149-65.

Munter, L. M., Voigt, P., Harmeier, A., Kaden, D., Gottschalk, K. E., Weise, C., Pipkorn, R., Schaefer, M., Langosch, D. & Multhaup, G. 2007. **GxxxG motifs within the amyloid precursor protein transmembrane sequence are critical for the etiology of Abeta42**. *EMBO J,* 26**,** 1702-12.

Ninomiya, H., Roch, J. M., Sundsmo, M. P., Otero, D. A. & Saitoh, T. 1993. **Amino acid sequence RERMS represents the active domain of amyloid beta/A4 protein precursor that promotes fibroblast growth**. *J Cell Biol,* 121**,** 879-86.

Nunan, J. & Small, D. H. 2000. **Regulation of APP cleavage by alpha-, beta- and gamma-secretases**. *FEBS Lett,* 483**,** 6-10.

Obregon, D., Hou, H., Deng, J., Giunta, B., Tian, J., Darlington, D., Shahaduzzaman, M., Zhu, Y., Mori, T., Mattson, M. P. & Tan, J. 2012. **Soluble amyloid precursor protein-alpha modulates beta-secretase activity and amyloid-beta generation**. *Nat Commun,* 3**,** 777.

Oh, S. Y., Ellenstein, A., Chen, C. D., Hinman, J. D., Berg, E. A., Costello, C. E., Yamin, R., Neve, R. L. & Abraham, C. R. 2005. **Amyloid precursor protein interacts with notch receptors**. *J Neurosci Res,* 82**,** 32-42.

Russell, M. J. B. a. R. B. 2003. *Bioinformatics for Genetic*, 291-314, Wiley.0-470-84393-4

Scheuermann, S., Hambsch, B., Hesse, L., Stumm, J., Schmidt, C., Beher, D., Bayer, T. A., Beyreuther, K. & Multhaup, G. 2001. **Homodimerization of amyloid precursor protein and its implication in the amyloidogenic pathway of Alzheimer's disease**. *J Biol Chem,* 276**,** 33923-9.

Sennvik, K., Fastbom, J., Blomberg, M., Wahlund, L. O., Winblad, B. & Benedikz, E. 2000. **Levels of alpha- and beta-secretase cleaved amyloid precursor protein in the cerebrospinal fluid of Alzheimer's disease patients**. *Neurosci Lett,* 278**,** 169-72.

Shaked, G. M., Kummer, M. P., Lu, D. C., Galvan, V., Bredesen, D. E. & Koo, E. H. 2006. **Abeta induces cell death by direct interaction with its cognate extracellular domain on APP (APP 597-624)**. *FASEB J,* 20**,** 1254-6.

Soba, P., Eggert, S., Wagner, K., Zentgraf, H., Siehl, K., Kreger, S., Lower, A., Langer, A., Merdes, G., Paro, R., Masters, C. L., Muller, U., Kins, S. & Beyreuther, K. 2005. **Homo- and heterodimerization of APP family members promotes intercellular adhesion**. *EMBO J,* 24**,** 3624-34.

Taylor, C. J., Ireland, D. R., Ballagh, I., Bourne, K., Marechal, N. M., Turner, P. R., Bilkey, D. K., Tate, W. P. & Abraham, W. C. 2008. **Endogenous secreted amyloid precursor protein-alpha regulates hippocampal NMDA receptor function, long-term potentiation and spatial memory**. *Neurobiol Dis,* 31**,** 250-60.

Thornton, E., Vink, R., Blumbergs, P. C. & Van Den Heuvel, C. 2006. **Soluble amyloid precursor protein alpha reduces neuronal injury and improves functional outcome following diffuse traumatic brain injury in rats**. *Brain Res,* 1094**,** 38-46.

Turner, P. R., Bourne, K., Garama, D., Carne, A., Abraham, W. C. & Tate, W. P. 2007. **Production, purification and functional validation of human secreted amyloid precursor proteins for use as neuropharmacological reagents**. *J Neurosci Methods,* 164**,** 68-74.

Tyler, S. J., Dawbarn, D., Wilcock, G. K. & Allen, S. J. 2002. **alpha- and beta-secretase: profound changes in Alzheimer's disease**. *Biochem Biophys Res Commun,* 299**,** 373-6.

Van Nostrand, W. E., Melchor, J. P., Keane, D. M., Saporito-Irwin, S. M., Romanov, G., Davis, J. & Xu, F. 2002. **Localization of a fibrillar amyloid beta-protein binding domain on its precursor**. *J Biol Chem,* 277**,** 36392-8.

Wimo, A. & Prince, M. 2010. World Alzheimer Report 2010 - The Global Economic Impact of Dementia. Available: http://www.alz.co.uk/research/files/WorldAlzheimerReport2010.pdf [Accessed 19.12.11].

Xue, Y., Lee, S. & Ha, Y. 2011. **Crystal structure of amyloid precursor-like protein 1 and heparin complex suggests a dual role of heparin in E2 dimerization**. *Proc Natl Acad Sci U S A,* 108**,** 16229-34.

Young-Pearse, T. L., Chen, A. C., Chang, R., Marquez, C. & Selkoe, D. J. 2008. **Secreted APP regulates the function of full-length APP in neurite outgrowth through interaction with integrin beta1**. *Neural Dev,* 3**,** 15.

Zhang, H., Ma, Q., Zhang, Y. W. & Xu, H. 2012. **Proteolytic processing of Alzheimer's beta-amyloid precursor protein**. *J Neurochem,* 120 Suppl 1**,** 9-21.

Zheng, H. & Koo, E. H. 2011. **Biology and pathophysiology of the amyloid precursor protein**. *Mol Neurodegener,* 6**,** 27.

Zhou, X., Hu, X., He, W., Tang, X., Shi, Q., Zhang, Z. & Yan, R. 2011. **Interaction between amyloid precursor protein and Nogo receptors regulates amyloid deposition**. *FASEB J,* 25**,** 3146-56.

Zou, K., Gong, J. S., Yanagisawa, K. & Michikawa, M. 2002. **A novel function of monomeric amyloid beta-protein serving as an antioxidant molecule against metal-induced oxidative damage**. *J Neurosci,* 22**,** 4833-41.

Appendix I

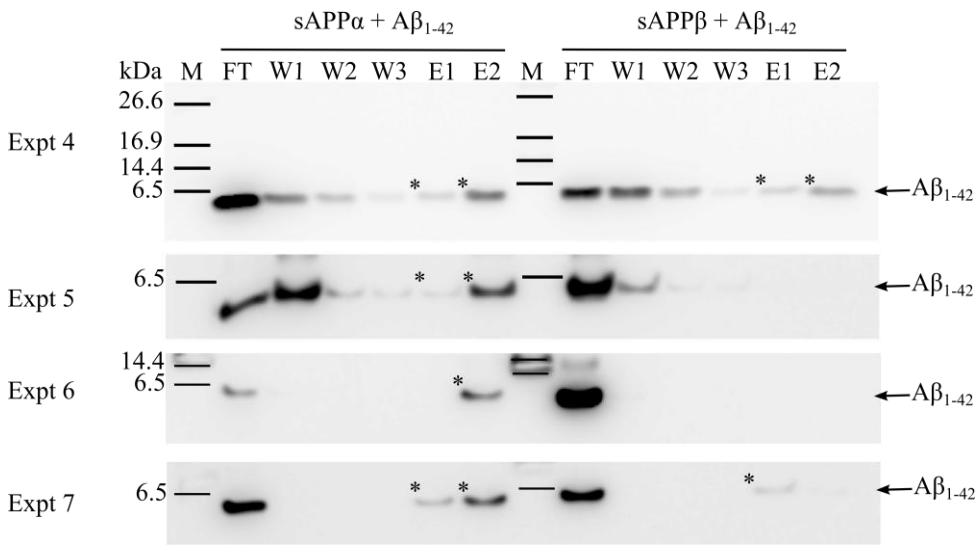

Figure 33: Western blotting with the anti-Aβ antibody 4G8 of four pull-down experiments (Expt 4, 5, 6, and 7), using sAPPα and sAPPβ as bait and $A\beta_{1-42}$ as prey. The *left* side illustrates the assays with sAPPα as bait, and the *right* side sAPPβ as bait. The asterisks indicate bound $A\beta_{1-42}$ showing much more $A\beta_{1-42}$ is bound to sAPPα than to sAPPβ. M. Peptide marker, FT: Flow through, W: Wash, E: Eluted protein fractions.

Appendix II

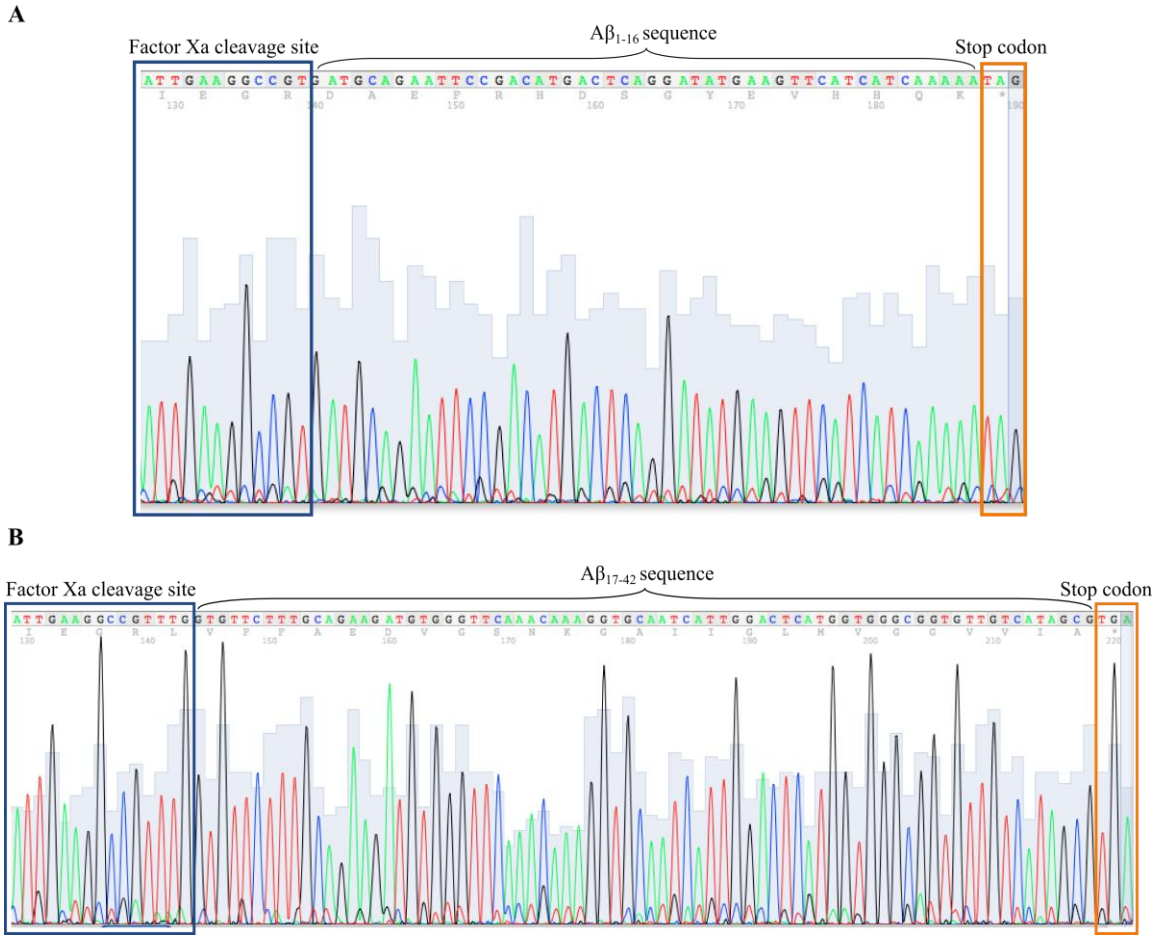

Figure 34: **A.** Sequencing results for $A\beta_{1-16}$, **B.** Sequencing results for $A\beta_{17-42}$. The blue box marks the Factor Xa cleavage site, the brackets indicate the $A\beta_{1-16}$ and $A\beta_{17-42}$ sequence, and the orange box marks the stop codon.

Appendix III

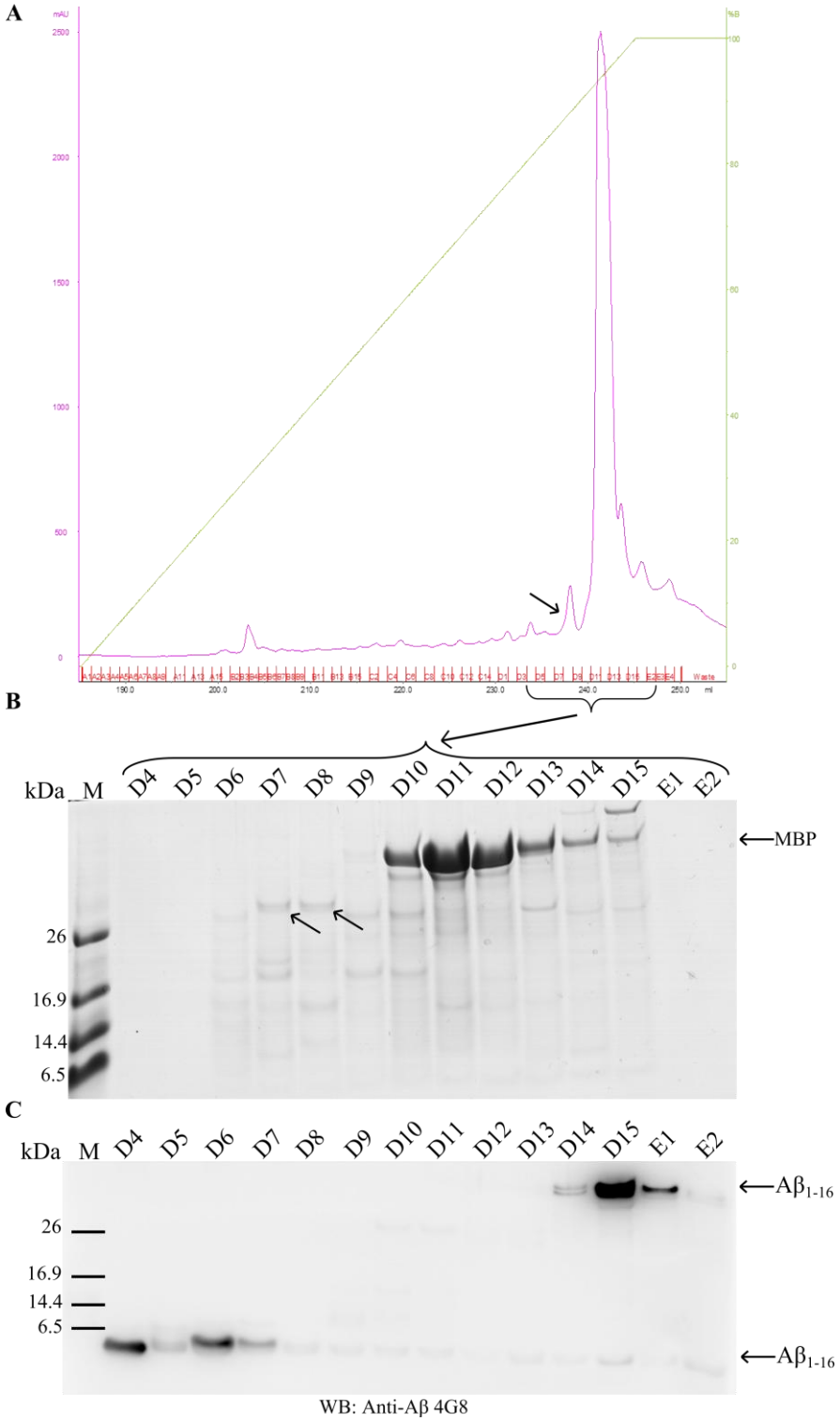

Figure 35: **A.** Fractionation of MBP and $A\beta_{1-16}$ on RPC. The pink trace illustrates the proteins absorbed at 215 nm, and the green trace is the percentage of buffer B which represents the change from 5-50 % acetonitrile. **B.** SDS-PAGE gel analysis of the fractions containing protein, and the flowthrough (FT), marked by the brackets on A. **C.** Western blotting with the anti-Aβ antibody 6E10 to confirm the identity of the protein. Fraction D4-D6 and D9 was pooled and used in the pull down assay. Fraction D14-D15 and E1-E2 contain uncleaved fusion protein.

Appendix IV

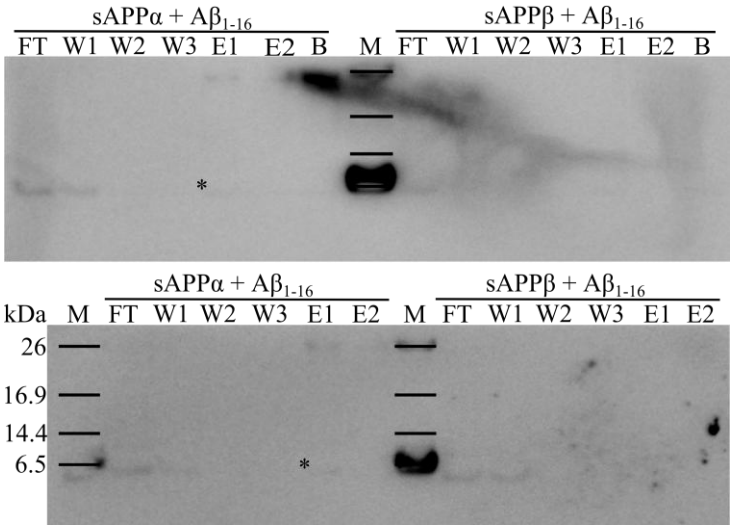

Figure 36: Western blots with the anti-Aβ antibody 6E10 of the 2nd and 3rd pull down assay using sAPPα and sAPPβ as bait and $Aβ_{1-16}$ as prey. The asterisks indicate bound $Aβ_{1-16}$. M: Peptide marker, FT: Flow through, W: Wash, E: Eluted protein fractions, B: Beads after elution of proteins.

Appendix V

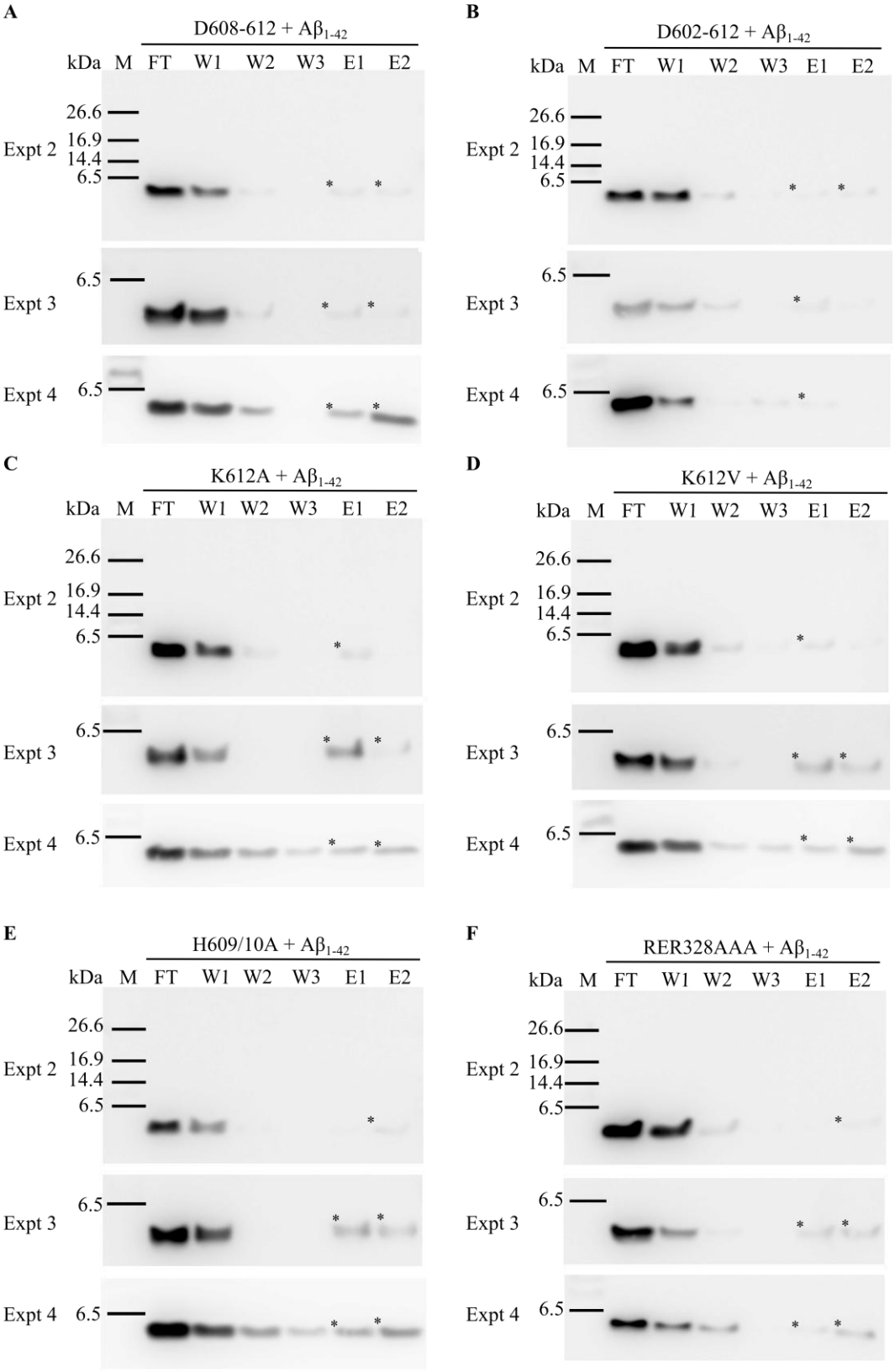

Figure 37: Western blotting with the anti-Aβ antibody 4G8 of three pull down experiments (expt 2, 3, 4) using the sAPPα variants as bait and $A\beta_{1-42}$ as prey: **A**. D608-612, **B**. D602-612, **C.** K612A, **D.** K612V, **E.** H609/10A, and **F.** RER328AAA . The asterisks indicate bound $A\beta_{1-42}$. M. Peptide marker, FT: Flow through, W: Wash, E: Eluted protein fractions.